



Assessment of the cooling capacity of plate tectonics and flood volcanism in the evolution of Earth, Mars and Venus

P. van Thienen*, N.J. Vlaar, A.P. van den Berg

Department of Theoretical Geophysics, University of Utrecht, P.O. Box 80.021, 3508 TA Utrecht, The Netherlands

Received 1 June 2004; received in revised form 29 November 2004; accepted 29 November 2004

Abstract

Geophysical arguments against plate tectonics in a hotter Earth, based on buoyancy considerations, require an alternative means of cooling the planet from its original hot state to the present situation. Such an alternative could be extensive flood volcanism in a more stagnant-lid like setting. Starting from the notion that all heat output of the Earth is through its surface, we have constructed two parametric models to evaluate the cooling characteristics of these two mechanisms: plate tectonics and basalt extrusion/flood volcanism. Our model results show that for a steadily (exponentially) cooling Earth, plate tectonics is capable of removing all the required heat at a rate of operation comparable to or even lower than its current rate of operation, contrary to earlier speculations. The extrusion mechanism may have been an important cooling agent in the early Earth, but requires global eruption rates two orders of magnitude greater than those of known Phanerozoic flood basalt provinces. This may not be a problem, since geological observations indicate that flood volcanism was both stronger and more ubiquitous in the early Earth. Because of its smaller size, Mars is capable of cooling conductively through its lithosphere at significant rates, and as a result may have cooled without an additional cooling mechanism. Venus, on the other hand, has required the operation of an additional cooling agent for probably every cooling phase of its possibly episodic history, with rates of activity comparable to those of the Earth.

© 2005 Elsevier B.V. All rights reserved.

Keywords: Terrestrial planets; Planetary cooling; Plate tectonics; Flood volcanism

1. Introduction

The literature of the past decades contains several examples of parameterized convection models for the secular cooling of the Earth during its history (e.g. Sharpe and Peltier, 1978; Davies, 1980; Turcotte, 1980; Spohn and Schubert, 1982; Christensen, 1985; Honda and Iwase, 1996; Yukutake, 2000). Depending on the parameters which are chosen, these models show vary-

* Corresponding author. Present address: Département de Géophysique Spatiale et Planétaire, Institut de Physique du Globe de Paris, 4 Avenue de Neptune, 94107 Saint-Maur-des-Fossés, France.

E-mail addresses: thienen@ipgp.jussieu.fr (P. van Thienen), vlaar@geo.uu.nl (N.J. Vlaar), berg@geo.uu.nl (A.P. van den Berg)

ing rates of cooling for the Earth. Similar models have been produced for Mars (e.g. Stevenson et al., 1983; Schubert and Spohn, 1990; Nimmo and Stevenson, 2000) and Venus (e.g. Solomatov and Zharkov, 1990; Parmentier and Hess, 1992). These are generally based on a power-law relation between the vigor of convection, represented by the thermal Rayleigh number, and the surface heat flow, represented by the Nusselt number. This latter corresponds to the transport of heat through the boundary between the solid and liquid/gaseous planetary spheres. In the modern Earth, this transport is part of the plate tectonic process, which in fact forms a quite efficient convective cooling mechanism (see Fig. 1a).

The early Earth, however, is thought to have been hotter by up to several hundreds of Kelvin (e.g. Nisbet et al., 1993). In a hotter Earth plate tectonics is counteracted by a thicker layering of oceanic crust and depleted crustal root produced in the melting process, remaining positively buoyant over very long times (Sleep and Windley, 1982), thus preventing subduction to take place (Vlaar, 1986; Vlaar and Van den Berg, 1991; Van Thienen et al., 2004b). Venus and Mars presently do not have plate tectonics (Nimmo and McKenzie, 1996; Zuber, 2001).

The timing of the initiation of modern style plate tectonics is still under debate. Whereas some authors interpret all observations on Archean cratons in a plate tectonic framework (De Wit, 1998; Kusky, 1998), others find the differences between the Archean granite-greenstone terrains and Phanerozoic tectonically active areas sufficiently large to discount plate tectonics as the mechanism of formation (Hamilton, 1998). The resulting range in estimates for the initiation of plate tectonics is 4.2–2.0 Ga. Ophiolites are considered to be obducted oceanic crust, and are therefore often used as a proxy for plate tectonics (e.g. Kusky et al., 2001). The oldest undisputed ophiolite sequences are about 2 Gyr old. The discovery of a 2.5 Ga ophiolite sequence in China (Kusky et al., 2001) has been disputed by others (Zhai et al., 2002).

An alternative mechanism to plate tectonics for the recycling of oceanic crust into the mantle may be the formation of eclogite in the deep lower parts of a thickened basaltic crust, which subsequently delaminates due to its intrinsic higher density. This process was modeled by Vlaar et al. (1994) and Van Thienen et al. (2004a). The upward transport of melts to produce a basaltic crust and the downward movement of earlier layers of basalt below this, together with delaminating

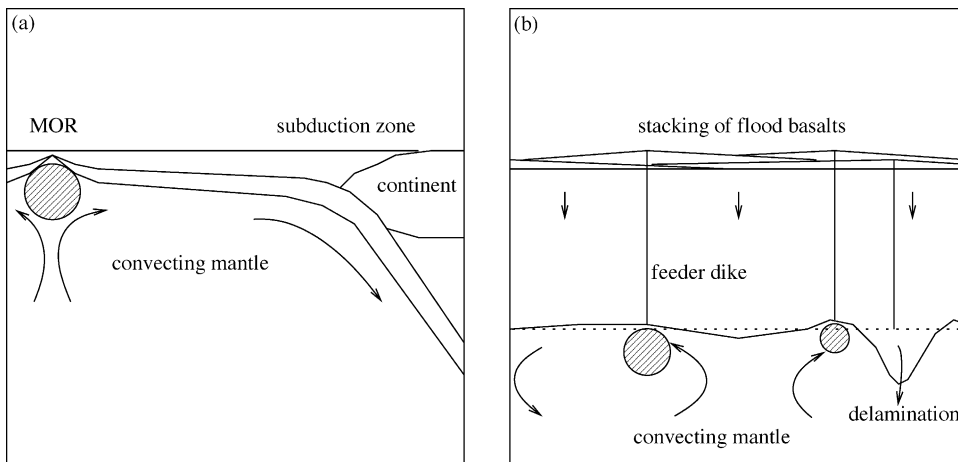


Fig. 1. Visualization of the plate tectonics and extrusion mechanisms. (a) Plate tectonics: a lithospheric column is produced at the mid-ocean ridge by partial melting of upwelling material (hatched area). As it moves towards the subduction zone, it cools down and the lithosphere thickens. At some point, the heat flow through the surface may match the mantle heat flow into the base of the lithosphere, and a steady state situation is reached. (b) Extrusion mechanism: Partial melting in the hot convecting mantle underneath the lithosphere (hatched areas) generates basaltic melts that migrate up to the surface, where they form flood basalts. As layer after layer of flood basalts is stacked onto the rest, lower crustal material may delaminate. Essentially the crust itself convects, upwards in the melt phase and downwards in the solid phase. Cooling takes place both by the advection of heat by the basalt and by conduction from the mantle through the lithosphere. The downward convection of the crust will decrease the conductive heat flux out of the mantle.

eclogite, in fact form a small scale convection cycle in the lithosphere itself (see Fig. 1b). The delamination of eclogite allows the upward flow of fertile material that can then melt and add more basalt to the crust. This in theory is a very efficient way of removing heat from the Earth, which involves the production and recycling of large volumes of basaltic crust. In non-plate tectonic settings, large volumes of basaltic magma may extrude as flood basalts and form so-called Large Igneous Provinces. These are common on Earth (Coffin and Eldholm, 1994), and more ubiquitous in the early Earth (Arndt, 1999; Abbott and Isley, 2002), and also common on Mars and Venus (Head and Coffin, 1997). Generally, these are associated with plume heads (e.g. White and McKenzie, 1995), but alternative interpretations which involve triggering from the lithosphere rather than the deep mantle have also been suggested (e.g. King and Anderson, 1995).

In this work we will evaluate the potential effect of both cooling mechanisms on the cooling history of the Earth, Mars and Venus. Reese et al. (1998) have also investigated the cooling efficiency of plate tectonics and stagnant lid regimes on Earth, Mars and Venus, using both boundary layer analysis and numerical models.

Our approach is different in two ways from many other studies:

1. Where many other papers apply parametric models to obtain model cooling histories of Earth, Mars or Venus, we approach the problem of planetary cooling from the opposite direction, by calculating the rate of operation of the two mechanisms for any reasonable combination of mantle temperature and cooling rate during the histories of the planets. As the exact cooling history of the terrestrial planets remains unknown, we construct several model cooling histories that are then evaluated in the framework of the two cooling mechanisms described above. This allows us to estimate the rates of activity of the mechanisms in the early planetary histories, which can be linked to geological observations.
2. We do not apply relations between Rayleigh number Ra and Nusselt number Nu stemming from boundary layer theory, but develop an alternative model formulation based on the fact that all heat which is removed from a planet must come through its surface. The reason for this is that although boundary layer theory gives very good results in stagnant

lid regimes and also for small-scale circulation at the base of oceanic lithospheres, there are some fundamental problems when applying it to the two regimes we propose to model on a global scale.

The main problem, applicable to both regimes, is the fact that the $Ra-Nu$ relations applied do not consider the effects of chemistry on buoyancy, which is the driving force of convection. As partial melting and associated compositional differentiation in planetary mantles significantly affects densities, this is an important parameter for the buoyancy of lithosphere (Oxburgh and Parmentier, 1977; Sleep and Windley, 1982; Vlaar and Van den Berg, 1991; Parmentier and Hess, 1992; Van Thienen et al., 2004b). Our approach circumvents this problem by not considering convection explicitly.

An additional serious difficulty with applying boundary layer theory in our flood volcanism model is the fact that at high extrusion rates, the geotherm may be significantly affected, as will be shown below, reducing the conductive heat flow out of the mantle.

In our models, the amount of activity required to obtain a certain cooling rate is determined as a function of potential temperature. More specifically, in the case of plate tectonics, we determine how fast it must operate to generate a certain planetary mantle cooling rate. We express this rate of operation with a parameter we call the turnover time τ , which indicates the average lifetime of oceanic lithosphere from creation at a mid-ocean ridge to its removal from the planetary surface and return into the mantle at a subduction zone. In the case of flood volcanism, we ascertain the average volumetric rate of basalt production, expressed as an equivalent layer thickness added to the global surface area (or an active fraction of this) per unit time: the extrusion rate δ .

2. Numerical model

For the two different geodynamical regimes described above we apply two different numerical models. The first, concerning the plate tectonics regime, is presented in Section 2.1. The second, which concerns the basalt extrusion mechanism, will be treated in Section 2.2.

The basic heat balance equation is applied to both models:

$$C \frac{d}{dt} \langle T \rangle = H_T - Q \quad (1)$$

with

$$C = \int_V \rho c_p dV \quad (2)$$

$$H_T = \int_V H dV \quad (3)$$

$$Q = \int_{\delta V} \vec{q} \cdot \vec{n} dA = Q_{\text{surf}} - Q_{\text{core}} \quad (4)$$

The symbols are explained in Table 1. Note that for a uniform value of ρc_p as applied here, $\langle T \rangle$ is the volume averaged temperature. The heat fluxes through the top and bottom boundaries of the model are combined in the term Q of Eq. (4). The Q_{surf} -term is different for the two mechanisms that are studied. The definition of this term for each mechanism will be given below. The total heat flux out of the mantle is treated separately in the following sections. The core heat flux into the mantle is used as an input parameter, and the choice of its value will be discussed below in Section 2.3. The internal heating due to the decay of radioactive elements is represented by H_T in Eq. (3).

Although Eq. (1) describes the rate of change of the volume averaged temperature of the mantle, we want to express the results in terms of potential mantle temperature. Therefore, we have obtained a simple relation between the rates of change of the volume averaged and potential temperatures. This relation was determined by volume integration in a spherical shell of several synthetic geotherms (adiabatic profile at depth and linear profile in top 100 km). The resulting expression, showing excellent correlation ($R > 0.999$), is:

$$\frac{d}{dt} \langle T \rangle = f_{T_{\text{avg}}} \frac{d}{dt} T_{\text{pot}} \quad (5)$$

The scaling factor $f_{T_{\text{avg}}}$ is different for the different planets because of size effects. The values are listed in Table 2.

To simplify the formulation of the problem, we assume that all heat transport from the mantle to the surface takes place in oceanic environments for plate tectonics. This is justified for the Earth by computing the magnitude of the continental mantle heat flow: eighty-

Table 1
Symbol definitions

Symbol	Parameter	Definition	Value/unit
A	Surface area		m^2
C	Mantle heat capacity		J K^{-1}
c_p	Specific heat		$\text{J kg}^{-1} \text{K}^{-1}$
d_{lith}	Lithosphere thickness		m
f	Active fraction of surface area		–
k	Thermal conductivity	$\kappa \rho c_p$	$\text{W m}^{-1} \text{K}^{-1}$
H	Radiogenic heating rate		W m^{-3}
H_T	Mantle radiogenic heating rate		W
N	Number of oceanic ridges		–
\vec{n}	Normal vector		–
n	Order of plate model series		–
Q	Heat flux		W
Q_{core}	Core heat flux		W
Q_{surf}	Surface heat flux		W
\vec{q}	Heat flow	$-k \nabla T$	W m^{-2}
q_0	Surface heat flow	$-k \frac{dT}{dz}$	W m^{-2}
R	Planetary radius		km
R_{core}	Core radius		km
T	Temperature		$^{\circ}\text{C}$
T_{pot}	Potential temperature		$^{\circ}\text{C}$
T_{surf}	Surface temperature		$^{\circ}\text{C}$
t	Time/age		s
u	Half spreading rate		m s^{-1}
\vec{u}	Velocity		m s^{-1}
V	Volume		m^3
w	Vertical velocity		m s^{-1}
YL_0	Plate thickness		m
δ	Extrusion rate		m s^{-1}
θ	Latitude		Radians
κ	Thermal diffusivity		$\text{m}^2 \text{s}^{-1}$
ρ	Density		kg m^{-3}
τ	Turnover time		s
ϕ	Angle/longitude		Radians

six percent of the present continental heat flux is accounted for by radiogenic heating, 58% of which is generated in the continental crust itself (Vacquier, 1998). Since about 30% of the global heat flux is through continental areas (Sclater et al., 1980; Pollack et al., 1993), this means that 15% of the current global heat flux is mantle heat (both radiogenic heat from the mantle and heat from mantle cooling) flowing through continental areas. We expect this fraction to be significantly smaller for the earlier Earth, because of the higher radiogenic heat production (causing a stronger blanketing effect) accompanied by a smaller amount of continental area relative to the oceanic domain. Furthermore, thicker roots of Archean cratons compared to post-Archean continental roots may divert mantle heat from the cratons (Davies, 1979; Ballard and Pollack, 1987, 1988).

Table 2

Values for the planetary radius R , core radius R_{core} , average mantle specific heat c_{pm} , gravitational acceleration g_0 , surface temperature T_{surf} , planetary mass M , relative silicate mantle mass M_{sm}/M , average mantle density $\langle \rho_{\text{m}} \rangle$, core heat flux Q_{core} and temperature scaling term $f_{T_{\text{avg}}}$ (see text) used in the calculations for Earth, Mars and Venus

Property	Earth	Mars	Venus
R (km)	6371	3397	6052
R_{core} (km)	3480	1700 ^{(1),(2),(3)}	3400 ⁽⁴⁾
c_{pm} ($\text{J kg}^{-1} \text{K}^{-1}$)	1250 ⁽⁵⁾	1250 ⁽⁵⁾	1250 ⁽⁵⁾
g_0 (m s^{-2})	9.81 ⁽⁶⁾	3.7 ⁽⁶⁾	8.9 ⁽⁶⁾
T_{surf} ($^{\circ}\text{C}$)	15 ⁽⁶⁾	-55 ⁽⁶⁾	457 ⁽⁶⁾
M (kg)		$6.42 \times 10^{23(6)}$	
M_{sm}/M		0.75 ⁽²⁾	
$\langle \rho_{\text{m}} \rangle$ (kg m^{-3})	4462 ⁽⁶⁾	3350	4234 ⁽⁴⁾
Q_{core} (TW)	$3.5 - 10^{(7),(8)}$	0.4 ⁽⁹⁾	0
$f_{T_{\text{avg}}}$	1.30	0.997	1.23

The average mantle density for Mars is calculated using planetary mass, silicate mantle mass fraction, and planetary and core size. References are: (1) Folkner et al. (1997), (2) Sanloup et al. (1999), (3) Yoder et al. (2003), (4) Zhang and Zhang (1995), (5) based on data from Fei et al. (1991), Saxena (1996), and Stixrude and Cohen (1993), (6) Turcotte and Schubert (2002), (7) Sleep (1990), (8) Anderson (2002), (9) heat flow from Nimmo and Stevenson (2000) for a 1700 km core.

For the extrusion models, we assume activity over the entire surface of the planets, since extensive volcanism on Earth also occurs in both continental (flood volcanism) and oceanic (plateaus) environments. Because both Venus and Mars do not have clearly distinguishable oceanic and continental areas, no continents will be taken into account for these planets.

2.1. Plate tectonics

In order to obtain an expression for the global surface heat flux Q_{surf} for the plate tectonics model, we use a plate model approximation (Carslaw and Jaeger, 1959; McKenzie, 1967; Turcotte and Schubert, 2002). This describes the development of the oceanic surface heat flow, dropping from a high initial value to an equilibrium value far from the ridge, where the surface heat flow is balanced by the mantle heat flow into the base of the lithosphere. In more complex models, this is explicitly associated with small-scale sublithospheric convection (Doin and Fleitout, 1996; Dumoulin et al., 2001). However, the parameter of interest in this work, the surface heat flow, shows nearly identical values

for the plate model and the more complex CHABLIS and modified CHABLIS models of Doin and Fleitout (1996) and Dumoulin et al. (2001), although the plate model shows slightly lower values for young oceanic lithosphere, since the heat flow through the base of the lithosphere increases more slowly. The surface heat flow for this plate model is given by the following equation:

$$q_0(t) = \frac{k(T_1 - T_0)}{y_{L0}} \left[1 + 2 \sum_{n=1}^{\infty} \exp\left(-\frac{\kappa n^2 \pi^2 t}{y_{L0}^2}\right) \right] \quad (6)$$

In this equation, q_0 is the surface heat flow, k the thermal conductivity, T_0 and T_1 the surface and basal plate temperatures, y_{L0} the plate thickness, κ the thermal diffusivity and $t = x/u_0$ the age of the lithosphere (see Table 1), where x is the distance to the spreading ridge and u_0 the constant half spreading velocity.

In order to obtain the global surface heat flux, we need to integrate this equation over the entire planet's oceanic surface, and to do this we make some assumptions on the geometry of the system.

We consider a spherical planet that is divided in pole to pole segments. These are separated by subduction zones and continents and each has a central spreading ridge. The boundaries and ridges may be offset by transform faults, which will not influence the argumentation (see Fig. 2). If such a segment has a longitudinal extent ϕ , its surface area A_s equals

$$A_s = 2\phi R^2 \quad (7)$$

We define the average time required to renew all oceanic crust as the turnover time τ . If we assume a fraction f of the entire planet's surface to be oceanic, i.e. involved in the plate tectonics system, divided in N segments of equal size, we can compute the turnover time τ by dividing the active surface area by the time derivative of the segment surface area:

$$\tau = \frac{4\pi R^2 f}{dA_s/dt} = \frac{4\pi R^2 f}{2NR^2(d\phi/dt)} = \frac{2\pi f}{N(d\phi/dt)} \quad (8)$$

which gives us

$$\frac{d\phi}{dt} = \frac{2\pi f}{N\tau} \quad (9)$$

In this framework, the lithospheric age t in Eq. (6) can be rewritten:

$$t = \frac{x}{u} = \frac{\phi R \cos \theta}{1/2(d\phi/dt)R \cos \theta} = \frac{\phi}{1/2(d\phi/dt)} \quad (10)$$

with x is the distance from the ridge, ϕ the corresponding longitudinal extent, θ the latitude and u the half spreading rate (hence the factor 1/2 in the denominator of this expression). We now compute the global oceanic heat flux by integrating Eq. (6) over the entire oceanic surface. This is done by considering $2N$ sections of oceanic crust from ridge to subduction zone, that have a longitudinal extent of

$$\phi_n = \frac{1}{2} \frac{2\pi f}{N} \quad (11)$$

The global oceanic heat flux now becomes

$$\begin{aligned} Q_{\text{surf}} &= 2N \int_{\phi=0}^{\pi f/N} \int_{\theta=0}^{\pi} \frac{k\Delta T}{y_{L0}} \\ &\times \left[1 + 2 \sum_{n=1}^{\infty} \exp\left(-\frac{\kappa n^2 \pi^2}{y_{L0}^2} \frac{\phi}{1/2(d\phi/dt)}\right) \right] \\ &\times R^2 \sin \theta d\theta d\phi \quad (12) \end{aligned}$$

Inserting Eq. (9) and integrating over θ gives

$$\begin{aligned} Q_{\text{surf}} &= 2N \int_{\phi=0}^{\pi f/N} \frac{2k\Delta TR^2}{y_{L0}} \\ &\times \left[1 + 2 \sum_{n=1}^{\infty} \exp\left(-\frac{n^2 \pi \kappa N \tau \phi}{y_{L0}^2 f}\right) \right] d\phi \\ &= \frac{4k\Delta TR^2 \pi f}{y_{L0}} \left\{ 1 + 2 \sum_{n=1}^{\infty} \frac{y_{L0}^2}{\pi^2 n^2 \tau \kappa} \right. \\ &\times \left. \left[1 - \exp\left(-\frac{n^2 \kappa \tau \pi^2}{y_{L0}^2}\right) \right] \right\} \quad (13) \end{aligned}$$

Note that the number of ridges N has disappeared from the equation, although Q_{surf} depends on the number of segments N implicitly through τ . As Eq. (8) shows, τ can be constant when simultaneously changing both N and $d\phi/dt$ keeping $N(d\phi/dt)$ constant. In other words, a smaller number of ridges requires a higher spreading rate to obtain the same turnover time. Although the applied geometry only allows for integer values of N , we will allow it to have non-integer values

as well, allowing a continuous range of possible global ridge lengths.

2.2. Extrusion mechanism

In the extrusion mechanism, we assume that, on long-term average, material is erupted and spreads out over the entire planetary surface. This is a simplification which ignores the fact that flood volcanism is generally a localized event, even for large Precambrian events, which cover at least ‘only’ 14–18% of the Earth’s surface (Abbott and Isley, 2002). Furthermore, associated with the extrusive flood basalts, intrusive rocks have been inferred (though not observed) to be at least as voluminous (Coffin and Eldholm, 1994), at least for the Earth, which are not included in the model. However, the cooling effect of extrusive compared to intrusive rocks may be expected to be greater due to the significantly smaller time scale of heat loss of these rocks and the possible blanketing effect of intrusives which may reduce the conductive heat flow out of the mantle.

We define the rate at which material is erupted as the extrusion rate δ , which indicates the time derivative of the extruded volume divided by the planetary surface area, or in other words the production of an equivalent thickness of crust per unit time. As all material that is extruded is stacked on top of existing crust in our model, pre-existing crustal material moves downward relative to the surface at the same rate as material is extruded, comparable to the permeable boundary approach of Monnereau and Dubuffet (2002) applied to Io. When (crustal) material reaches the depth of the lithosphere thickness, defined below in Section 2.3, we assume it to delaminate (see Fig. 1b). It must be noted here that this mechanism differs from stagnant lid convection in the sense that the continuous stacking of material on top of the lithosphere has a significant influence on the geotherm and therefore the conductive heat flux through the lithosphere (see Fig. 3). Therefore, scaling law relations which provide excellent predictions of heat flow for stagnant lid settings (e.g. Reese et al., 1998; Solomatov and Moresi, 2000), may not be applied here. Furthermore, the advection of heat (including latent heat) by magma migrating to the surface is the primary means of mantle cooling in the regions of parameter space which we will focus on, and conductive cooling as in the stagnant lid regime of secondary

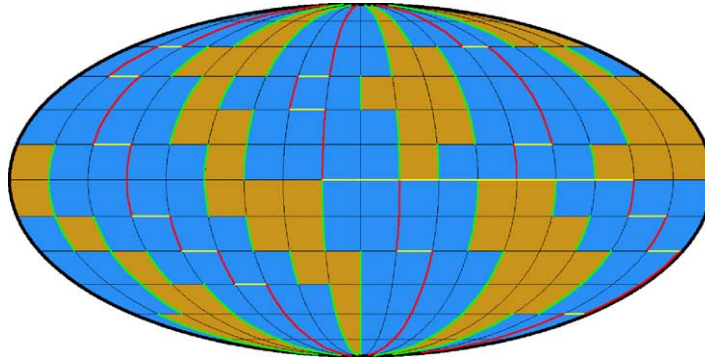


Fig. 2. Conceptual visualization of the parameterization of plate tectonics as described in Section 2.1 in a Mollweide projection, for a situation in which three oceans ($N = 3$) cover two thirds of the Earth's surface area. All oceans (blue) have the same uniform longitudinal extent ϕ , are bounded by subduction zones (green) at active continental (brown) margins, and have mid-ocean ridges (red) in the middle. Transform faults (yellow) may offset the ridge and consequently also the margin of the oceans. Note that only the transform faults connecting parts of ridge axes have been drawn.

importance. For the extrusion model, the surface heat flux Q_{surf} in Eq. (1) consists of two parts. The first is the heat advected by magma that is extruded onto the surface. We assume the magma to lose all its internal excess heat to the hydrosphere/atmosphere, taking on the surface temperature. We note, however, that lava flow cooling in the dense Venusian atmosphere may be less efficient (by 30–40%) than on Earth (Snyder, 2002). The heat flux from this component is described by:

$$Q_{\text{extru}} = 4\pi R^2 f(\delta\rho c_p \delta T + \delta T_m \Delta S \rho_m) \quad (14)$$

In this expression, f is the fraction of the planetary surface on which the mechanism is active, δ is the extrusion rate, ρ the density of the solidified magma, δT the temperature drop of the magma from the potential temperature to the surface temperature, T_m the mantle temperature below the lithosphere, ΔS the latent heat of melting and ρ_m the mantle density (see Tables 1 and 2). In this approximation, the advection term (first bracketed term) assumes that the partial melt has the same temperature as the mantle prior to melting, thus neglecting the fact that latent heat consumption during partial melting has lowered its temperature, which results in a small overestimate of the amount of heat removed from the mantle. The reduction of the temperature of the matrix by latent heat consumption is accounted for in the second bracketed term. Hauck and Phillips (2002) demonstrated that this may be a significant term in the thermal evolution of planets. The second component

of the surface heat flux is the conductive heat flux out of the mantle. Because in this scenario, there is continuous stacking of successive extrusive units, crustal material is continuously pushed downward. As we assume a constant lithosphere thickness (for a fixed potential temperature) and a fixed temperature at the lower boundary of the lithosphere corresponding to the temperature of the mantle adiabat of given potential temperature T_{pot} , this causes an increase in the geothermal gradient in the deep lithosphere and a decrease at shallow levels (see Fig. 3). In order to quantify this, we use a 1D finite difference model of the thermal state of the lithosphere. We consider the heat equation:

$$\rho c_p \left(\frac{\partial T}{\partial t} + \vec{u} \cdot \nabla T \right) = k \partial_j \partial_j T + H \quad (15)$$

Steady state geotherms are assumed, and we simplify the equation to one dimension:

$$\rho c_p w \frac{\partial T}{\partial z} = k \frac{\partial^2 T}{\partial z^2} + H \quad (16)$$

In this equation, the extrusion of basalt is represented by the vertical velocity w , which we define to be equal in magnitude to the extrusion rate δ . Eq. (16) is written down for constant and uniform thermal conductivity. However, work by Hofmeister (1999) shows that the thermal conductivity may vary significantly for the range of pressures and temperatures found in the mantle. Numerical models of Van den Berg and Yuen (2002) and Van den Berg et al. (2002) show that this effect may

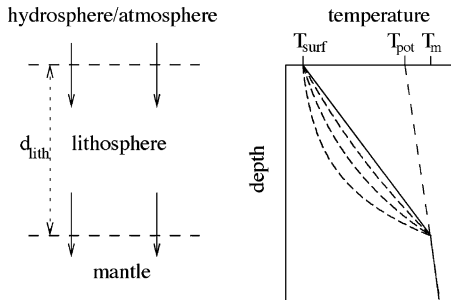


Fig. 3. ‘Lithospheric convection’ in which, at the top boundary, material is added by magma extrusion and at the bottom boundary material is lost due to delamination, resulting in a constant lithosphere thickness. Geotherms are computed for this setting using expression (16) in a finite difference scheme, see text. For a situation without radiogenic heating, the trivial case of $w = \delta = 0$ (no extrusion and delamination) results in a linear geotherm (solid curve). For a finite downward velocity, the geotherm is deflected (dashed curves, for $w = \delta = 100, 250$ and 500 mMyr^{-1}), resulting in a significantly decreased conductive heat flux through the lithosphere.

significantly delay mantle cooling, resulting in higher mantle temperatures. A higher melt production due to a thinning of the lithosphere relative to a constant conductivity case was observed in numerical models by Hauck and Phillips (2002). However, in smaller-scale models applied to oceanic lithosphere, Honda and Yuen (2001) find that although the thermal structure of the lithosphere is affected by a variable thermal conductivity relative to a constant conductivity case, the oceanic heat flow is not significantly influenced.

We solve Eq. (16) numerically for the lithosphere, defined below in Section 2.3, with the surface temperature and the potential temperature extrapolated to the base of the lithosphere as boundary conditions. A finite difference scheme (using 400 nodes for the lithosphere) is used to obtain the geotherm and from this the conductive heat flux at the top of the lithosphere Q_{bl} , out of the mantle (see Fig. 3).

Together the two components form the total surface heat flux:

$$Q_{\text{surf}} = Q_{\text{extru}} + Q_{bl} \quad (17)$$

2.3. Input parameters

The main input parameters for the different planets are listed in Table 2. The least constrained parameter in the models is the heat flux from the core into the mantle. Recent estimates for the present-day Earth

range from 2.0 to 12 TW (Sleep, 1990; Anderson, 2002; Buffett, 2003). The former estimate is based on hotspot fluxes interpreted as associated with mantle plumes originating at the core mantle boundary (CMB) and, as Labrosse (2002) argues, is probably a lower limit because not all plumes that start at the CMB would make it to the surface. The latter is based on an evaluation of mantle heat transfer mechanisms near the CMB (Anderson, 2002; Buffett, 2003). Estimates for the core heat flux during the (early) history of the Earth are even more difficult to make. Thermal evolution calculations by Yukutake (2000) show the core heat flux decreasing from 12 TW at 4.4 Ga to a present value of 7.5 TW. A decreasing value is also found in the models of Labrosse et al. (1997). Buffett (2003) calculated that in the early Earth, before the formation of an inner core (the timing of which is uncertain, but in the range of 1.9–3.2 Ga, Yukutake, 2000), a core heat flux of about 15 TW would be required to drive the geodynamo. However, an increase of the core heat flux during the history of the Earth also seems plausible. Large temperature contrasts over the D'' layer (δT about 1200 K, Anderson, 2002) have been inferred suggesting slow heat transfer from the core. Recent results of numerical mantle convection modeling including temperature and pressure dependent thermal conductivity show a core heat flux fluctuating around a slightly increasing value and a temperature contrast across the bottom boundary layer increasing with time, showing the mantle to cool faster than the core, in line with planetary cooling from the top down (Van den Berg et al., 2004).

It is even more difficult to estimate the core heat fluxes for Mars and Venus. Nimmo and Stevenson (2000) reasoned that, as a superadiabatic temperature gradient is required to drive convection, the maximum obtainable conductive heat flow would be realized along an adiabatic thermal gradient. They estimated this number for the Martian core to be $5\text{--}19 \text{ mWm}^{-2}$. The absence of a magnetic field suggests that the martian core does not convect and therefore this number may be an upper limit for the current martian core heat flow. Using a value of 10 mWm^{-2} and a core radius of 1700 km (see Table 2), this results in a core heat flux of 0.4 TW. For Venus, the adiabatic conductive heat flow would be $11\text{--}30 \text{ mWm}^{-2}$ (Nimmo, 2002). However, the calculations of Turcotte (1995), Phillips and Hansen (1998) and Nimmo (2002) indicate that the mantle of Venus may be heating up and the core heat

flux would therefore be declining. We will therefore not consider a core heat flux for Venus in our calculations.

Other input parameters that are not well constrained are the thickness of the cooling plate (in the plate model, used in the plate tectonics formulation, see Section 2.1) and the lithosphere (used in the extrusion model, see Section 2.2) as a function of potential temperature. The plate thickness does not directly correspond to a physical thickness of crust or lithosphere, but it is an empirical parameter which describes the behavior of heat transport. In our model, it is obtained by matching the plate model heat flow with oceanic heat flow values obtained from numerical convection models (see Appendix A) in the same way as a plate model is fitted to heat flow observations from the ocean floor in e.g. Parsons and Sclater (1977). In the extrusion model, the (thermal) lithospheric thickness is defined by the 1327 °C (1600 K) isotherm (Turcotte and Schubert, 2002). Solomatov and Moresi (2000) show that in a stagnant lid setting, the temperature difference across the rheological sublayer depends on the internal temperature. This results in a varying isotherm defining the lithosphere thickness. However, we use a simpler approach, choosing a fixed value of 1327 °C (1600 K) for the isotherm bounding the lithosphere. Below we test the sensitivity of the results to the lithosphere thickness. Since the rheology of mantle material is strongly temperature dependent (e.g. Karato and Wu, 1993), the thickness of the (rheological) lithosphere is a function of the potential mantle temperature. We have obtained a parameterization for both the plate thickness in the plate tectonics model and the lithospheric thickness in the extrusion model using 2D numerical convection models, see Appendix A and B.

The resulting expression for the effective plate thickness y_{L0} is

$$y_{L0} = 147.4 - 0.1453T_{\text{pot}} + 2.077 \times 10^{-4}T_{\text{pot}}^2 - 8.333 \times 10^{-8}T_{\text{pot}}^3 \quad (18)$$

with y_{L0} in km and T_{pot} in °C. This expression gives an effective plate thickness of just under 125 km for the present day potential temperature of 1350 °C. This is consistent with results of Parsons and Sclater (1977), but somewhat thicker than the 100 km found by Stein and Stein (1992).

The resulting parameterization for the lithosphere thickness as a function of potential temperature is:

$$d_{\text{lith}} = 6684 - 9.7352T_{\text{pot}} + 4.7675 \times 10^{-3}T_{\text{pot}}^2 - 7.8049 \times 10^{-7}T_{\text{pot}}^3 \quad (19)$$

with d_{lith} in km and the potential temperature T_{pot} in °C.

We investigate the sensitivity of the results to the plate and lithosphere thickness, the core heat flux, the internal heating rate and the oceanic surface fraction in Sections 3.3 and 3.9. In a more general planetary context, we also investigate the effect of gravitational acceleration, planet size in Sections 3.7 and 3.12. We expect the Earth's and the martian surface temperature to have varied over less than 100 K during most of their histories. Venus, however, may have experience variations over several 100 K (Bullock and Grinspoon, 2001; Phillips et al., 2001). Therefore, we also investigate the sensitivity of our results to surface temperature in Sections 3.7 and 3.12.

The average mantle densities for Earth and Mars are calculated by dividing mantle mass over volume. In the case of Venus, we use the average of the results of two four-zone hydrostatic models by Zhang and Zhang (1995). The average heat capacities of the planetary mantles have been computed using data from Fei et al. (1991), Stixrude and Cohen (1993) and Saxena (1996). Since all values fall in the range of 1200–1300 J kg⁻¹ K⁻¹, a uniform value of 1250 J kg⁻¹ K⁻¹ is applied.

2.4. Solving the equations

In the plate tectonics scenario, we solve Eq. (1) for the turnover time τ using Eq. (13) for the surface heat flux. This means we obtain the turnover time that is required to facilitate a specified cooling rate at a specified potential temperature.

In the extrusion mechanism case, we solve Eq. (1) for the extrusion rate δ , using Eqs. (14) and (17) to obtain the corresponding surface heat flux, which gives us the required extrusion rate to obtain the specified cooling rate at the specified potential temperature.

In both cases, the parameter we want to solve for is not easily isolated from the equations. We therefore apply a bisection algorithm to compute the desired solutions numerically (see Table 3).

Table 3

Numerical scheme which is used for solving the volume averaged heat Eq. (1), either for the plate tectonics model, in which case ξ indicates the turnover time τ , or for the flood volcanism case, where ξ indicates the extrusion rate δ

Step	Action
0	Prescribe potential temperature and cooling rate for this experiment prescribe lower and upper boundary for ξ ($\xi_{lb}^{(0)}$ and $\xi_{ub}^{(0)}$) spanning the range in which the value of ξ is expected; start loop with iteration counter $n = 1$
1	Compute $\xi_{bis}^{(n)} = (\xi_{lb}^{(n-1)} + \xi_{ub}^{(n-1)})/2$
2	Compute $dT_{pot}/dt _{bis} = dT_{pot}/dt(\xi_{bis}^{(n)})$
3	Compare $dT_{pot}/dt _{bis}$ to prescribed dT_{pot}/dt ; if relative mismatch $< \epsilon_{bis}$, $\xi = \xi_{bis}^{(n)}$ and loop ends
4	If $dT_{pot}/dt _{bis} < dT_{pot}/dt$, ξ must be greater than $\xi_{bis}^{(n)} \rightarrow$ increase lower boundary of search domain: $\xi_{lb}^{(n+1)} = \xi_{bis}^{(n)}$ If $dT_{pot}/dt _{bis} > dT_{pot}/dt$, ξ must be less than $\xi_{bis}^{(n)} \rightarrow$ decrease upper boundary of search domain: $\xi_{ub}^{(n+1)} = \xi_{bis}^{(n)}$
5	$n = n + 1$ and return to step 1

3. Results

3.1. Mantle cooling rates

Results obtained from the models described in the previous sections are presented below. These results quantify the characteristics of the two cooling mechanisms, plate tectonics and flood volcanism, for specific cooling histories. Since the applied models represent quasi steady states, they do not tell us anything about the cooling histories of the Earth, Mars and Venus themselves. In this section, we first explore the range of plausible cooling histories in T_{pot} , dT_{pot}/dt -space, using simple parameterizations of two types of plausible cooling behavior. These scenarios will then be included in (the discussion of) the figures presenting the results of the model calculations as described in the previous sections, and aid the discussion of the results that may be relevant for the cooling histories of the terrestrial planets. Many parameterized convection models in the literature show planetary cooling curves which show a long-term monotonically decreasing cooling rate (e.g. Honda and Iwase, 1996), resulting from the power-law relation between cooling rate (through the Nusselt number) and internal temperature (through the Rayleigh number) which is the basis of these models. These characteristics of a decaying cooling rate are ap-

proximated by a simple exponential expression, and therefore we will approximate long-term decaying secular cooling using an exponential cooling curve. Short-term cooling pulses will be viewed separately. Fig. 4a shows five cooling histories in which a simple exponential cooling is assumed from a starting temperature of 1500–1900 °C at 4.0 Ga to the Earth's present estimated potential temperature of 1350 °C. They were constructed by imposing the start and end points to the expression

$$T = T_0 \exp(at) \quad (20)$$

for which the corresponding cooling rate is

$$\frac{dT}{dt} = aT_0 \exp(at) \quad (21)$$

Markers are included at 200 Myr intervals to indicate the passing of time. These model cooling histories through T_{pot} , dT_{pot}/dt -space will be used below in the discussion of the results as reference models. The initial temperatures shown seem to cover the range of temperatures inferred for the early Archean Earth mantle, and thus the area spanned by these curves contains plausible cooling histories for a steadily cooling Earth with an exponential decay of both the potential temperature and the cooling rate. We note, however, that possibly very high melt fractions associated with the high end of our temperature range may affect the dynamics in ways that are not well represented by our models. Because of the assumed similar formation histories and sizes of Mars and Venus compared to the Earth, we assume the same mantle temperature window to be valid for these two planets.

In order to be able to compare our results to those of well-known parameterized mantle convection models based on a Rayleigh–Nusselt relation, we show thermal evolution curves for Ra – Nu models for plate tectonics and stagnant lid regimes, based on the formalism of Reese et al. (1998), in the same representation as used for the exponential curves in Fig. 4b (see caption for details). A number of models is within the area of our exponential curves. Some models start at a higher cooling rate but rapidly (some hundreds of Myear) converge to the range of the exponential curves, indicated by the shaded region in Fig. 4b, which represents a zoom-out of Fig. 4a. Some other models show a period of heating before cooling sets in. High cooling rates during initial phases of cooling are also observed in numeri-

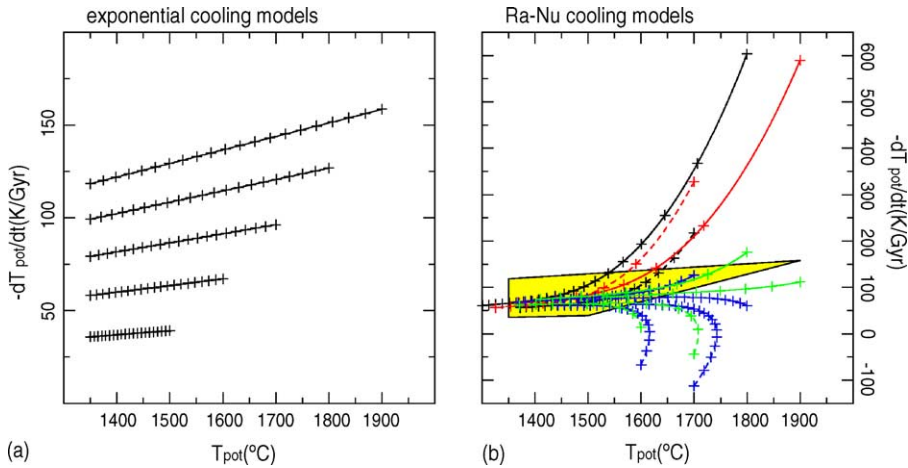


Fig. 4. (a) Exponential cooling curves in T_{pot} , dT_{pot}/dt -space, for starting temperatures of 1500, 1600, 1700, 1800 and 1900 °C. (b) Cooling curves in T_{pot} , dT_{pot}/dt -space for parametric mantle convection models (2D aspect ratio 1 domain) based on a $Ra-Nu$ relation. These curves were obtained by combining Eqs. (15), (39), (61) and (62) of Reese et al. (1998) with the heat balance Eq. (1). Internal heating was applied consistent with the models of the present paper, and a zero core heat flux was prescribed. Of a range of models, only those with final temperatures between 1300 and 1600 °C were selected. Explanation of the colours: black—Earth, plate tectonics model; blue—Earth, stagnant lid model; red—Mars, plate tectonics model; green—Mars, stagnant lid model. Solid and dashed lines indicate different viscosity models (Newtonian, temperature dependent, activation enthalpy 300 kJ/mol) with $\eta = 10^{20}$ Pas at 2000 K (solid) and $\eta = 10^{21}$ Pas at 2000 K (dashed). The yellow area represents the curve range of frame (a). Note that in these models, T_{pot} equals the internal temperature T_i as they do not include adiabatic compression. In both frames, markers are 200 Myr apart.

cal mantle convection models, e.g. those by Van den Berg and Yuen (2002), which show fluctuating cooling rates with peak values of 300–500 K Gyr⁻¹ during the early histories of their experiments. If the cooling of the planets is not an exponentially decaying process, or if the system diverges from this behavior from time to time as in an episodic scenario, cooling rates may be significantly higher than those shown in Fig. 4a. In Fig. 5, we show maximum cooling rates that are obtained for a Gaussian shaped pulse in the cooling rate (Fig. 5a and b). Fig. 5c shows the temperature drop of the mantle caused by this cooling pulse on the horizontal axis. On the vertical axis, the duration of the cooling pulse ($\pm 2\sigma$) is indicated. Obviously high cooling rates are expected for short pulses with a large temperature drop, and lower cooling rates for longer pulses with smaller temperature drops. Nearly everywhere in this figure, the cooling rates are significantly higher than in the steady exponential cooling of Fig. 4a. Below, we will present the results of our models for conditions spanning the range of the cooling curves for both the exponential models of Fig. 4a and the Ra-Nu models of Fig. 4b, and part of those of the upper left part of Fig. 5c.

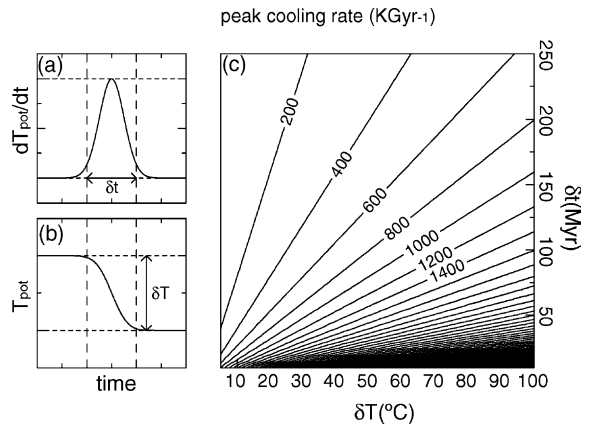


Fig. 5. Peak cooling rates for mantle cooling pulses with Gaussian shape using arbitrary units (left hand side frames). The corresponding temperature drop is indicated on the horizontal axis, and the vertical axis signifies the duration ($\pm 2\sigma$) of the cooling pulse.

3.2. Plate tectonics on Earth

The computed results for the plate tectonics model described in Section 2.1 applied to the Earth are presented in Fig. 6a–d, showing contour levels of the

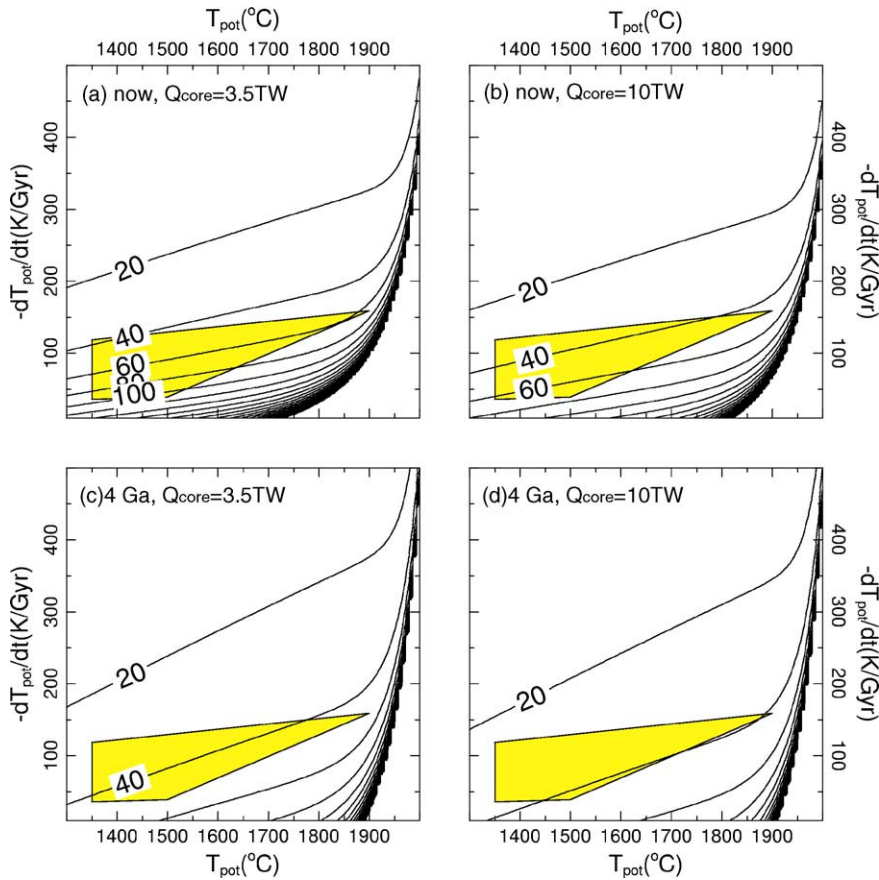


Fig. 6. Results of the plate tectonics model for a core heat fluxes of 3.5 and 10 TW for the present-day and early Earth (in terms of radiogenic heat production rate and extent of the continents). Contours indicate the turnover time τ (in Myear) as a function of potential temperature (horizontal axis) and cooling rate (vertical axis). The shaded zone corresponds to the region spanned by the exponential cooling curves of Fig. 4, and are thus representative of steady state secular cooling. Higher values on the vertical axis may be caused by cooling pulses (see Fig. 5).

turnover time τ , for the present situation and for a case representing the early Earth (4 Ga) and for two different values for the core heat flux, 3.5 and 10 TW. The timings are based on the rate of internal heating ($4.8 \times 10^{-12} \text{ W kg}^{-1}$ for the present and $14.4 \times 10^{-12} \text{ W kg}^{-1}$ for the early Earth) and the (estimated) extent of the continents ($f = 0.63$ for the present and $f = 0.97$ for the early Earth, McCulloch and Bennett, 1994). All four frames show the potential temperature of the mantle on the horizontal axis, and the mantle cooling rate on the vertical axis (in K G yr^{-1}). The contours indicate the turnover time τ that is required to maintain a cooling rate at a potential temperature corresponding to the position in the diagram. The shaded

area indicates the region occupied by the exponential cooling histories shown in Fig. 4a, with the present-day Earth plotting near the left hand vertical boundary of this region. Note that Fig. 6a–d are two sets of sections through two 3D boxes, in which the internal heating rate is plotted on the third axis. In such a 3D representation, it is possible to track any cooling history independent of the internal heating rate, whereas in 2-D sections such as those of Fig. 6a,b and c,d (and also other figures below), any cooling history tracked in an individual frame is for a fixed internal heating rate. Because such a 3D representation is difficult to bring across in 2D figures, we use the 2D sections and keep this caveat in mind. The core heat fluxes represent

the range of values found in the literature as discussed in Section 2.3.

From these diagrams we observe that *for a fixed cooling rate*, a longer turnover time is required at higher mantle potential temperatures. This is a result of the decreased plate thickness at higher potential temperatures. Small-scale sublithospheric convection keeps the base of the lithosphere at a constant temperature (conductive cooling is the slowest step of the process). This results in an increase in the conductive surface heat flow, and therefore a reduction of the advective heat flow that is required to maintain the specified cooling rate. For a constant mantle potential temperature, obviously, higher cooling rates require a shorter turnover time. Each figure shows a region in the lower right hand side corner where required turnover times are more than 500 million years (which is the maximum contour plotted). In these regions heat conduction through a static lithosphere is essentially sufficient to generate the required rate of cooling. This is a combined effect of the low cooling rates that characterize this regime which is effectively a stagnant lid situation (Solomatov and Moresi, 1996) and a thin lithosphere which is the result of a high mantle potential temperature.

The range of turnover times allowed by our model results for the present-day Earth, assuming an exponential cooling model, is indicated in Fig. 6a–b by the left hand vertical boundary of the shaded area that envelopes the exponential cooling curves of Fig. 4a. Turnover times of about 30–90 Myr are permissible, consistent with the average age of subducting lithosphere on the present-day Earth of about 70 million years (Juteau and Maury, 1999, Table 11.1). For the early Earth, results consistent with exponential cooling indicate turnover times of about 40–50 million years (right hand side boundary of shaded area in Fig. 6c–d). The effect of an increased core heat flux is that the surface heat flux must also increase in order to obtain the same specified cooling rate and therefore the turnover time must decrease.

3.3. Sensitivity of plate tectonics results to the model parameters

Fig. 7 shows the sensitivity of the results of the previous section to changes in plate thickness, core heat

flux, internal heating rate and extent of the oceanic domain. In the experiments which produced these curves, all parameters were fixed (including the plate thickness, which in the previous experiments was a function of potential temperature following Eq. (18), see figure caption for values), except for the single parameter under investigation. In descending order of sensitivity, plate thickness, internal heating rate, oceanic surface fractional area and core heat flux influence the turnover time τ . There appears to be a threshold value for the importance of plate thickness. As Fig. 7a shows, for thicknesses of less than 60 km (corresponding to a potential mantle temperature of 1850 °C in expression (18)), the effect of changing the thickness is that the turnover time increases strongly at higher temperatures. This effect is stronger for a thinner plate. It is caused by thermal conduction through the lithosphere taking over from conductive cooling of the lithosphere itself as the most important cooling factor. Note that the threshold thickness will be slightly different for different cooling rates. However, above 60 km thickness, the effect of changing the thickness is minimal in the potential temperature range investigated. This means that the oceanic heat flow is dominated by the conductive cooling of the lithosphere from its hot initial state as it was formed at mid-ocean ridges. For Venus and Mars, discussed below, lithosphere thickness may be significantly greater than for Earth due to a possibly dryer mantle, which increases mantle viscosity (e.g. Nimmo and McKenzie, 1998). The curves of Fig. 7a shows that a thicker lithosphere does not significantly influence the turnover time τ , which validates our application of the Earth-based parameterization for plate thickness to Mars and Venus. The other parameters, core heat flux, internal heating rate and extent of the oceanic domain, have a more straightforward and linear effect, essentially scaling the turnover time more or less independently of the potential temperature (see Figs. 7b–d).

3.4. Application of the plate tectonics model to Mars and Venus

The plate tectonics model of Section 2.1 was also applied to Mars and Venus. The parameters that were adjusted to modify the model for these planets are the core and planetary radius (resulting in a different mantle heat capacity and surface to volume

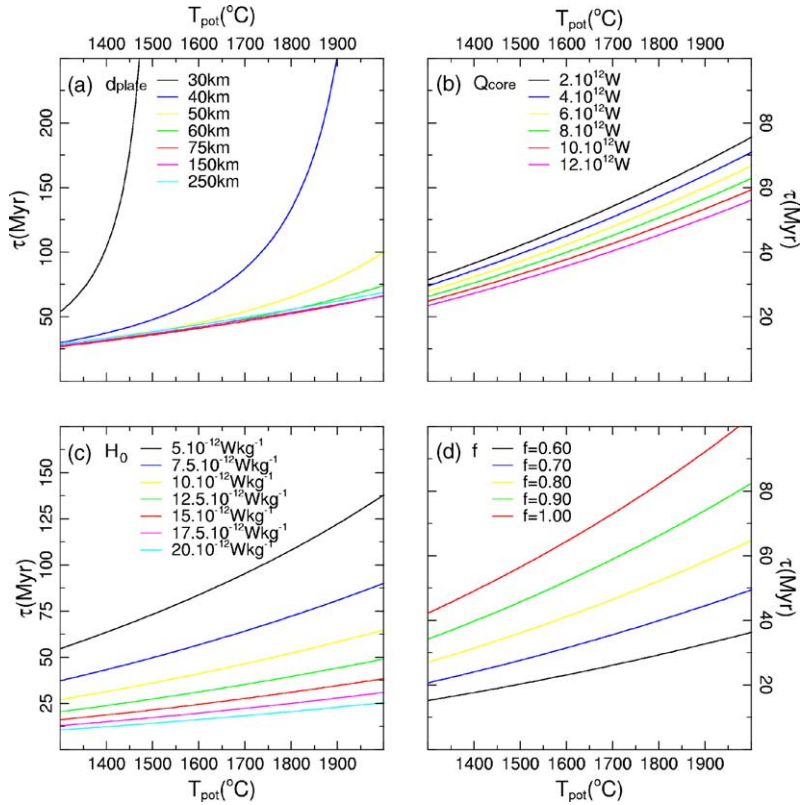


Fig. 7. Sensitivity tests of the plate tectonics model to single parameters. Fixed values of the non-varying parameters are: core heat flux $Q_{\text{core}} = 7 \text{ TW}$, plate thickness $d_{\text{plate}} = 100 \text{ km}$, internal heat productivity $H_0 = 10 \times 10^{-12} \text{ W kg}^{-1}$, oceanic surface fraction $f = 0.80$, mantle cooling rate $-dT_{\text{pot}}/dt = 100 \text{ K G yr}^{-1}$. The curves show the turnover time τ as a function of (a) plate thickness d_{plate} ; (b) core heat flux Q_{core} ; (c) internal heat productivity H_0 ; (d) extent of the active area f .

ratio), the surface temperature (controlling the surface heat flow), the average mantle density (controlling the mantle heat capacity), the core heat flux and the conversion factor between potential and volume averaged temperatures (resulting from different planetary radius and gravitational acceleration, which cause different adiabatic temperature profiles), using values listed in Table 2. Continents are assumed to be absent, so the oceanic surface fraction f is set to 1. The results of these experiments are shown in Fig. 8. Two different values for the internal heating rate were used, which we assume to represent the present ($H_0 = 4.80 \times 10^{-12} \text{ W kg}^{-1}$) and early ($H_0 = 14.40 \times 10^{-12} \text{ W kg}^{-1}$) states of the planets. Again, the range of reasonable exponential cooling curves of Fig. 4a is included as the shaded area.

3.5. Plate tectonics on Mars

For present-day Mars, shown in Fig. 8a, the results indicate that only extremely high cooling rates of more than 250 K G yr^{-1} require the operation of plate tectonics. For lower, more likely cooling rates, turnover times are well over 500 million years, which essentially means that conductive cooling is sufficient. This is a result of the fact that, compared to the Earth, surface to volume ratio ($\sim R^2/R^3$) is relatively large. This results in conductive cooling through a comparatively greater surface area (scaling with R^2 , see Eq. (13)) of a comparatively smaller heat reservoir (Eq. (2), scaling with R^3), which is more efficient. The same goes for early Mars (characterized in our model by an increased internal heating rate $H_0 = 14.40 \times 10^{-12} \text{ W kg}^{-1}$), shown in Fig. 8b, where the position of the planet may be ex-

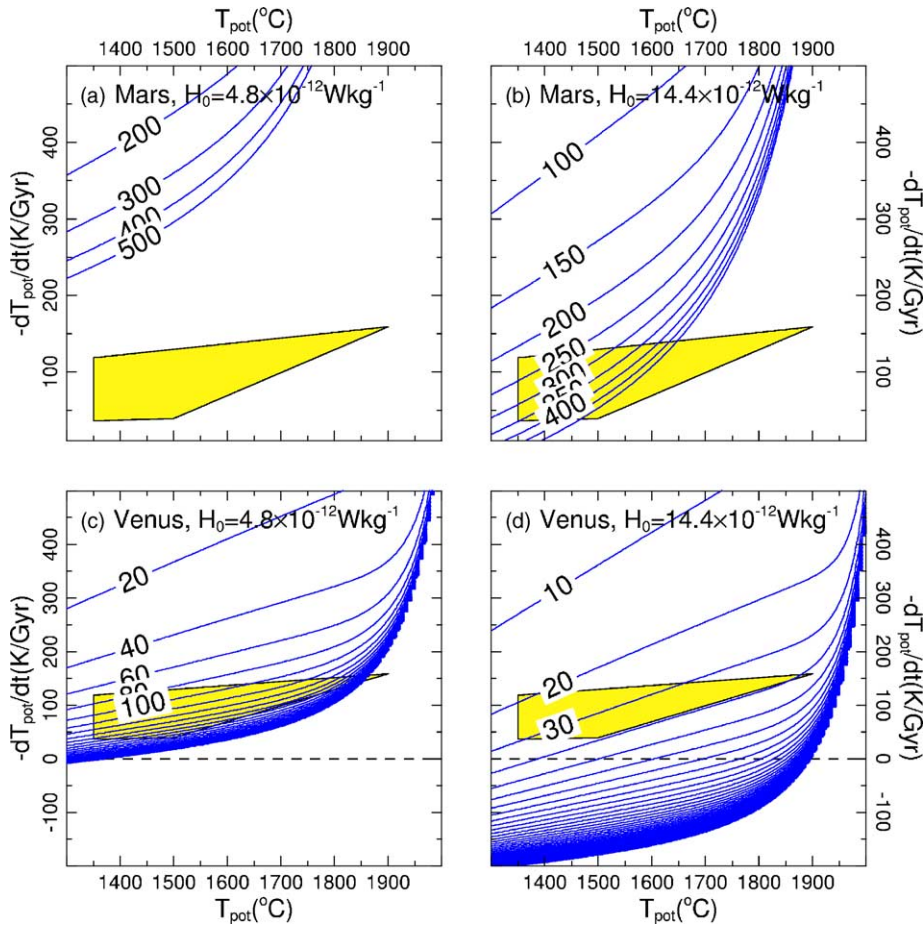


Fig. 8. Turnover time τ for Mars and Venus for models with internal heating rates of $4.80 \times 10^{-12} \text{ W kg}^{-1}$ and $14.40 \times 10^{-12} \text{ W kg}^{-1}$. For other model parameters (see Table 2). For an explanation of the figure see caption of Fig. 6.

pected in the right hand side of the frame due to a higher mantle temperature.

3.6. Plate tectonics on Venus

Venus, shown in Fig. 8c–d (present and early), shows more Earth-like characteristics (see Table 2). At a probable present potential temperature similar to that of the Earth of $1300 \text{ }^\circ\text{C}$ with an upper limit of $1500 \text{ }^\circ\text{C}$ (Nimmo and McKenzie, 1998), turnover times for hypothetical plate tectonics would be on the order of tens to some hundreds of million years if we assume an exponential cooling scenario. A more likely scenario in which short episodes of rapid cooling (see Fig. 5)

and longer episodes of stagnation alternate would require turnover times of only some tens of million years or less (upper left of Fig. 8c) in the cooling episodes and (many) hundreds of million years (lower left of this frame) during the stagnation periods. For early Venus, some cooling mechanism other than conduction definitely seems required (see Fig. 8d). If plate tectonics were this mechanism, turnover times on the order of some tens of million years are required, comparable to the results for the early Earth (Fig. 6c–d). Note that we have included negative values for the cooling rate, since Venus may be heating up at the moment (Phillips and Hansen, 1998; Nimmo, 2002) and may have had more heating episodes (Turcotte, 1995).

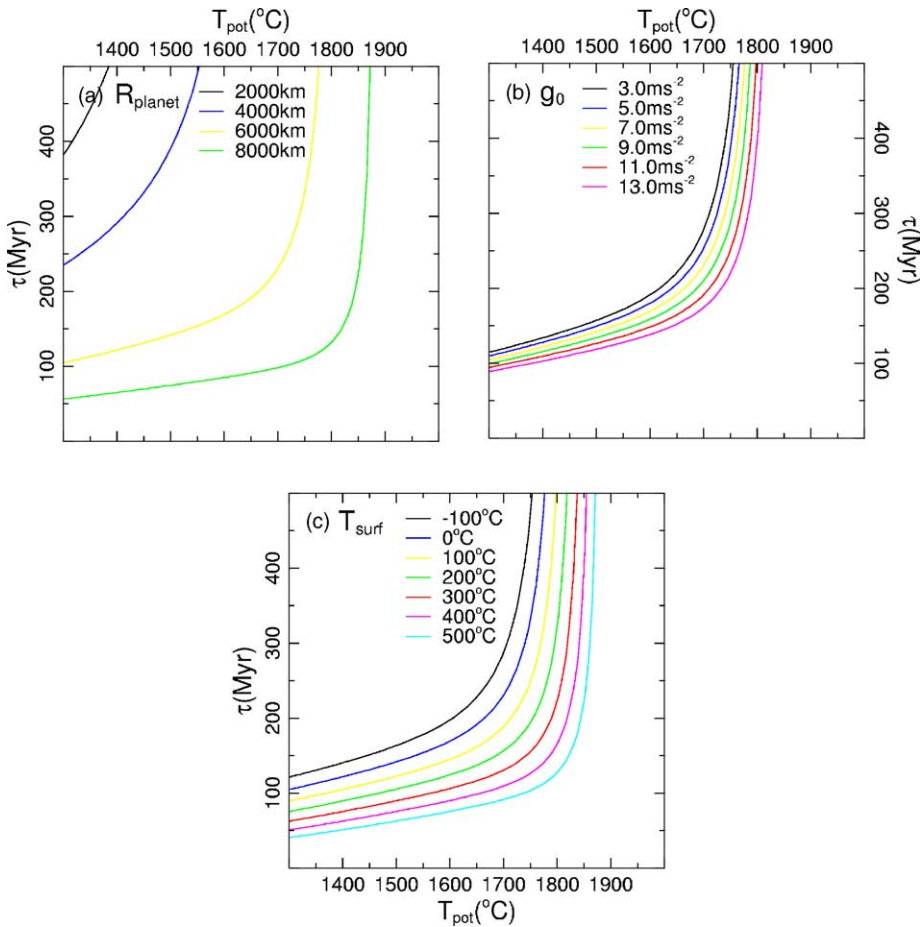


Fig. 9. Variation of the turnover time τ as a function of (a) planet size R_{planet} , (b) gravitational acceleration g_0 and (c) surface temperature T_0 . Values of non-varying parameters are $Q_{\text{core}} = 1 \text{ TW}$, $d_{\text{lith}} = 100 \text{ km}$, $H_0 = 4.8 \times 10^{-12} \text{ W kg}^{-1}$, $f = 0.80$, $-dT_{\text{pot}}/dt = 100 \text{ K G yr}^{-1}$, $g_0 = 7.0 \text{ ms}^{-2}$, $R = 6000 \text{ km}$. The core radius is half of the planetary radius in all cases. The potential to average temperature scaling factor $f_{T_{\text{avg}}}$ in Eq. (5) is recomputed for all different combinations of planet size and gravitational acceleration used.

3.7. Effects of planetary parameters on heat transfer by plate tectonics

In order to evaluate the effect of the different distinguishing parameters of the terrestrial planets separately, we have calculated the turnover time while varying one parameter (planetary radius, gravity or surface temperature) and keeping the others fixed. The results are shown in Fig. 9a–c for these three parameters, respectively, for a fixed cooling rate of 100 K G yr^{-1} (other parameters see figure caption). It is clear from this figure that the planet's size, through the surface area

to volume ratio ($\sim R^2/R^3$), dominates the cooling behavior of a planet, to such an extent that small planets can cool conductively at considerable rates, whereas larger planets need a more efficient cooling agent like plate tectonics to get a moderate cooling rate less than 100 K G yr^{-1} . The gravitational acceleration affects the adiabatic gradient ($\alpha g T/c_p$), but this effect is relatively minor. An elevated surface temperature which may be relevant for Venus during episodes of its history, tends to reduce the conductive heat flow, and therefore faster plate tectonics, if present, is required to maintain a certain rate of cooling.

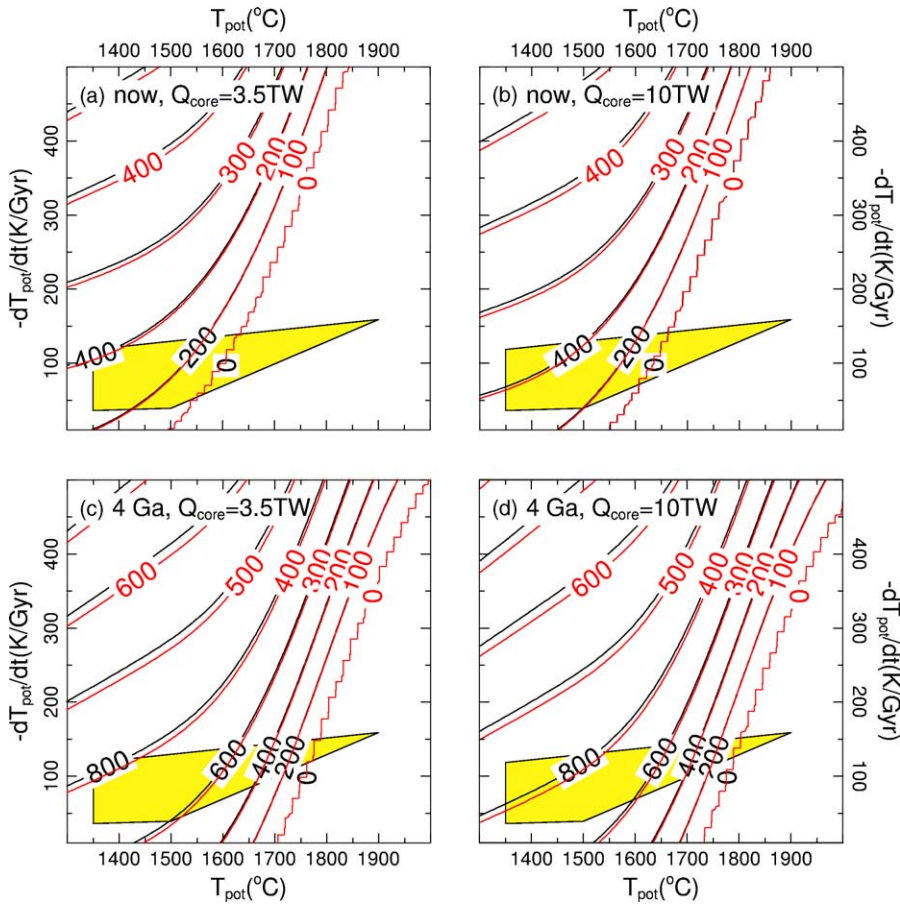


Fig. 10. Results of the extrusion model for a core heat fluxes of 3.5 and 10 TW for the present-day and early Earth (in terms of radiogenic heat production rate and extent of the continents). Black contours indicate the extrusion rate δ in mM yr^{-1} , representing the average thickness of basaltic crust produced per million years for the entire planetary surface. Red/grey contours indicate the global volumetric basalt production rate, in $\text{km}^3 \text{yr}^{-1}$.

3.8. Extrusion mechanism on Earth

Fig. 10 shows the results of the extrusion models. It is similar to Fig. 6, but it shows different quantities, the extrusion rate δ (black contours) in mM yr^{-1} and the global volumetric extrusion rate (red/grey contours) in $\text{km}^3 \text{yr}^{-1}$. The extrusion rate δ represents the global ($f = 1.0$) average thickness of basaltic crust produced in 1 million years. We consider this mechanism to operate globally (in contrast with plate tectonics), since continental flood volcanism is not uncommon. The extrusion rate δ and the global volumetric extrusion rate only differ by a factor of (surface area/1 Myr). Again, four cases are investigated, using

internal heating and continent extent values for the present ($H_0 = 4.80 \times 10^{-12} \text{ W kg}^{-1}$) and early (4 Ga, $H_0 = 14.40 \times 10^{-12} \text{ W kg}^{-1}$) Earth and two values for the core heat flux of 3.5 and 10 TW. The general trends are (1) a higher potential temperature reduces the lithosphere thickness and increases the temperature contrast over the lithosphere, thus increasing the conductive heat flux and decreasing the extrusion rate, (2) a higher cooling rate requires a greater extrusion rate, and (3) an increase in the internal heating rate (either radiogenic or from the core) requires an increase in the extrusion rate. For comparison, a rough estimate for the ‘extrusion rate’ of the present-day Earth is $\sim 20 \text{ km}^3 \text{yr}^{-1}$ (McKenzie and Bickle, 1988). This number is an order

of magnitude lower than the numbers presented in Fig. 10a and b (the left hand side boundary of the shaded area), although the mechanism is different. In Fig. 10c, the extrusion rate δ is below 0 above potential temperatures of 1800 for the exponential cooling curves (shaded area) in early Earth scenarios. This means that cooling through the lithosphere was sufficiently efficient to generate cooling without requiring magmatic processes. For lower potential temperatures, global volumetric extrusion rates may be more than an order of magnitude higher than for the present-day Earth, up to $350 \text{ km}^3 \text{ yr}^{-1}$. It is important to keep in mind that in our model, only extrusive material is considered. Although generally, few intrusive rocks are exposed in regions formed by flood volcanism on Earth, they are possibly at least as voluminous, up to several times as voluminous, as the extrusives (Coffin and Eldholm, 1994). Inspection of high resolution images of the walls of Valles Marineris reveals the presence of intrusive rocks on Mars as well (Williams et al., 2003), and though we have no observations to confirm this, there is no reason to believe they are absent on Venus. Intrusive rocks are significantly slower in releasing their heat to the surface than extrusives, but in doing so, their perturbation of the geotherm causes a thermal blanketing effect for the underlying lithosphere, reducing the heat flow out of the mantle. It may be expected that the volumetric extrusion rates, when interpreted as total crustal production rates, shown in Fig. 10 are somewhat higher when a significant part of the material is intruded rather than extruded.

3.9. Sensitivity of the extrusion mechanism heat transfer

The sensitivity of the extrusion rate δ to the lithosphere thickness (a), core heat flux (b), internal heating rate (c) and extent of the ‘oceanic’ domain (d) is shown in Fig. 11. Strong effects can be seen for low values of the lithosphere thickness, where sufficiently low values may result in completely conductive cooling (no extrusion required), and the internal heating rate. For a lithosphere thickness greater than about 100 km, there is no sensitivity of the extrusion rate δ to the lithosphere thickness, since conduction through the lithosphere plays a minor role. In the parameterization of the lithosphere thickness applied here (expression (19)), this transition corresponds to a potential temperature

of about 1600°C (see Fig. 15). Below this temperature, our assumption of the applicability of our Earth-based parameterization for the lithosphere thickness to Mars and Venus holds for higher mantle viscosities for these planets, which would increase the lithosphere thickness. For higher temperatures, the thickness computed from (19) may be too small for Mars or Venus, resulting in an underestimate of the extrusion rate δ . The effect of surface area (assuming that the extrusion mechanism is active on only a part of the planet’s surface) is smaller, and that of the core heat flux is quite limited in the parameter range that was investigated.

3.10. Extrusion mechanism on Mars

Fig. 12 shows the results of the extrusion model for Mars and Venus, for internal heating values assumed to represent the recent and early history, respectively, of these planets. The results for present-day Mars (Fig. 12a) at the estimated present location of Mars in $T_{\text{pot}}, dT/dt$ -space in the lower left hand side corner of the diagram indicate that only very limited volumetric extrusion rates are required for the cooling of Mars. Compared to Earth, the global volumetric extrusion rates are an order of magnitude smaller. In terms of extrusion rate δ , the difference is not as large due to the smaller surface area of Mars. Early Mars (Fig. 12b) also requires only a small global volumetric extrusion rate, even for very high cooling rates, due to a combination of thinner lithosphere compared to present-day Mars and large surface area to volume ratio compared to larger planets.

3.11. Extrusion mechanism on Venus

Things are quite different for Venus (Fig. 12c and d). When assuming an exponential time dependence of planetary cooling as indicated by the shaded area, which may not be correct for Venus, we see volumetric extrusion rates on the order of $100\text{--}200 \text{ km}^3 \text{ yr}^{-1}$, up to five times greater than the present-day Earth’s plate tectonics crustal production rate, and comparable to the rate that would be required for the present-day Earth if the extrusion mechanism were the main cooling agent (see Fig. 10a and b). Early Venus also shows model results similar to those of the early Earth (see Fig. 10c and d consistent with the similarity of the model parameters for both planets). Note that we have again

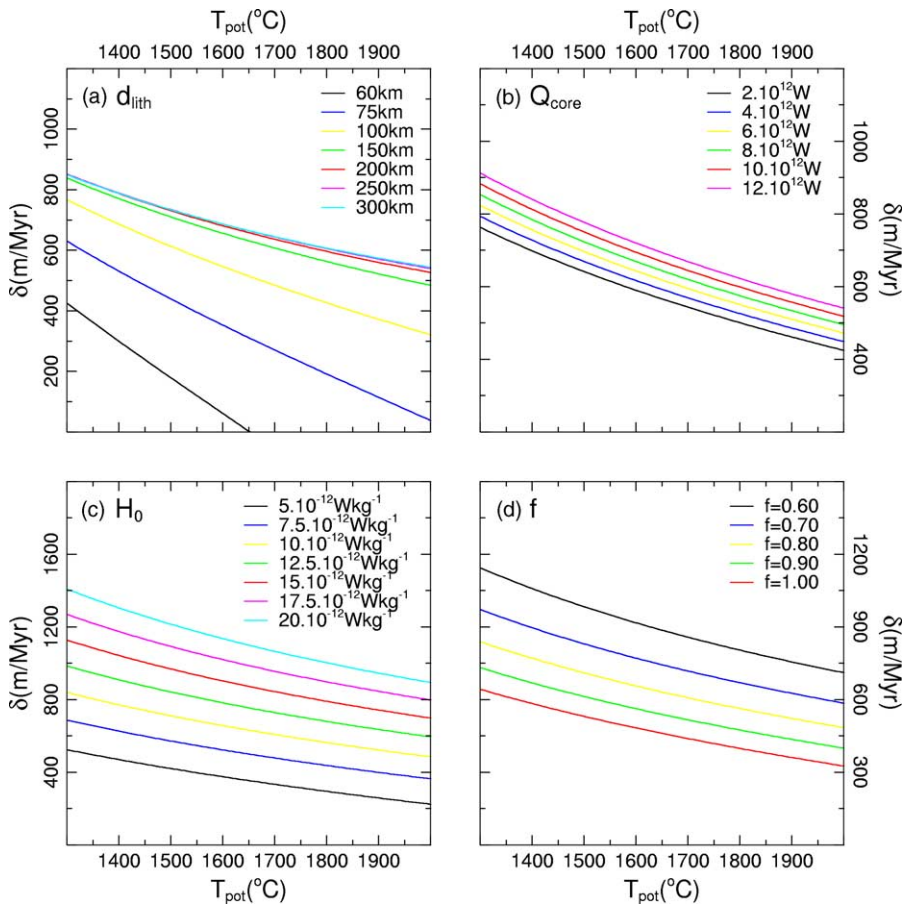


Fig. 11. Sensitivity tests of the extrusion model to single parameters. Fixed values of the non-varying parameters are: core heat flux $Q_{\text{core}} = 7 \text{ TW}$, lithosphere thickness $d_{\text{lith}} = 150 \text{ km}$, internal heat productivity $H_0 = 10 \times 10^{-12} \text{ W kg}^{-1}$, oceanic surface fraction $f = 0.80$, mantle cooling rate $-dT_{\text{pot}}/dt = 100 \text{ K G yr}^{-1}$. The curves show the extrusion rate δ as a function of (a) lithosphere thickness d_{lith} ; (b) core heat flux Q_{core} ; (c) internal heat productivity H_0 ; (d) extent of the active area f .

included negative values for the cooling rate to show the effect of possible periods of heating in the planet’s history.

3.12. Effects of planetary parameters on the extrusion mechanism heat transfer

For the extrusion mechanism, the sensitivity for planetary parameters is also investigated (Fig. 13). The presentation of the results is similar to that of the plate tectonics sensitivity tests of Fig. 9, and the parameter values are the same. An extra frame (d) has been added showing the sensitivity of the results to the value of the latent heat of melting. The results show that the

planetary size (using a fixed value for g_0 , which is rather artificial but the alternative would be to assume a relation between radius and gravitational acceleration, which is also artificial because of the dependence on composition), the surface temperature (as noted before, possibly of importance for Venus), and the latent heat of melting may strongly affect the extrusion rate required for a prescribed cooling rate. The first affects the planetary cooling efficiency through the surface area to volume ratio, and the second is a factor in the temperature gradient over the lithosphere, determining the conductive heat transport. The latent heat effect scales linearly with the extrusion rate. The gravitational acceleration, affecting the adiabatic gradient, has a

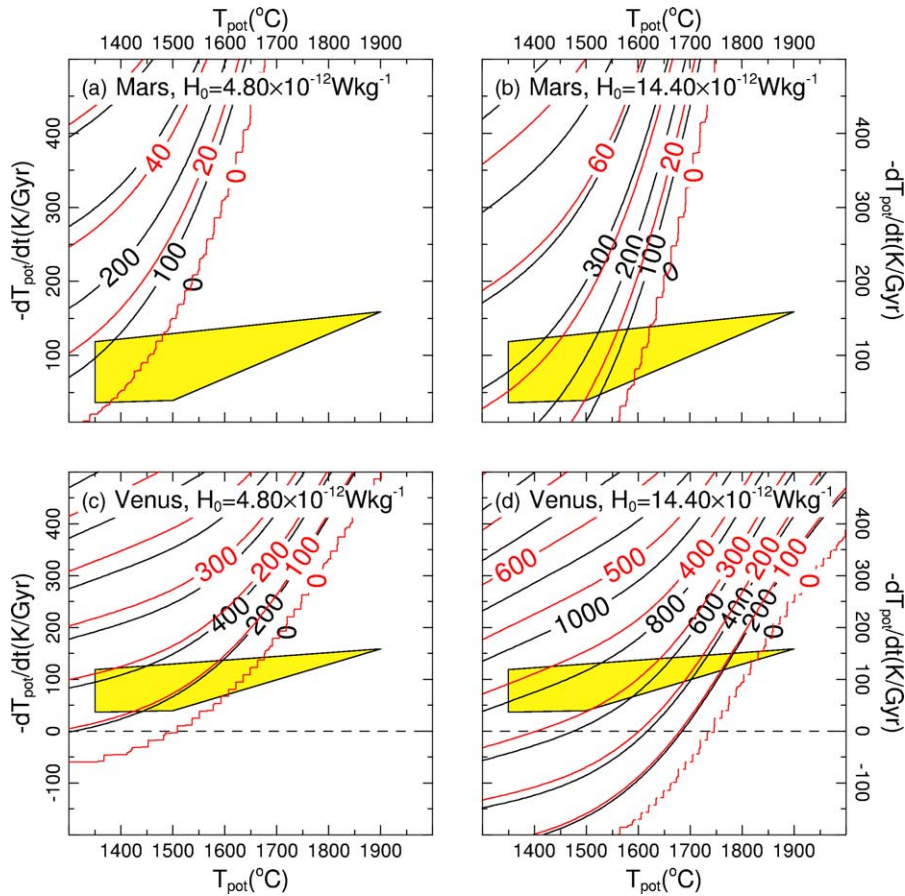


Fig. 12. Results of the extrusion model for Mars and Venus, using two different values for the internal heating rate representing the recent and early histories of the planets. Black contours indicate the extrusion rate δ in mM yr^{-1} , representing the average thickness of basaltic crust produced per million years for the entire planetary surface area. Red/grey contours indicate the global volumetric basalt production rate, in $\text{km}^3 \text{yr}^{-1}$.

limited effect, but obviously R_{planet} and g_0 are coupled quantities.

3.13. Comparison with Ra – Nu cooling models

The approach presented in the present paper is different from that applied in many parametric cooling models based on Ra – Nu relations (see above) in the sense that we do not consider the driving forces of the dynamics and therefore do not directly predict rates of operation. Therefore, direct comparison of our results to those of Ra – Nu models is impossible. We can however consider the thermal evolutions of those models in the context of our results. The Ra – Nu cooling curves

presented in Fig. 4b for the plate tectonics parameterization (black for Earth/Venus, red for Mars) show rapid cooling and, when compared to Figs. 6c and d and 8c and d, high rates of operation during the initial 0.4–1.0 Gyr, corresponding to turnover times which may be less than 20 Myr. However, as noted above, the fact that the Ra – Nu models do not take into account the chemical component of the driving force of plate tectonics (and apply other simplifications), this may not be realistic. When comparing stagnant lid Ra – Nu models to our extrusion models, it must first be noted that these two classes of models are not identical in terms of heat transport mechanism: the models of Fig. 4b are purely conductive (though other workers have

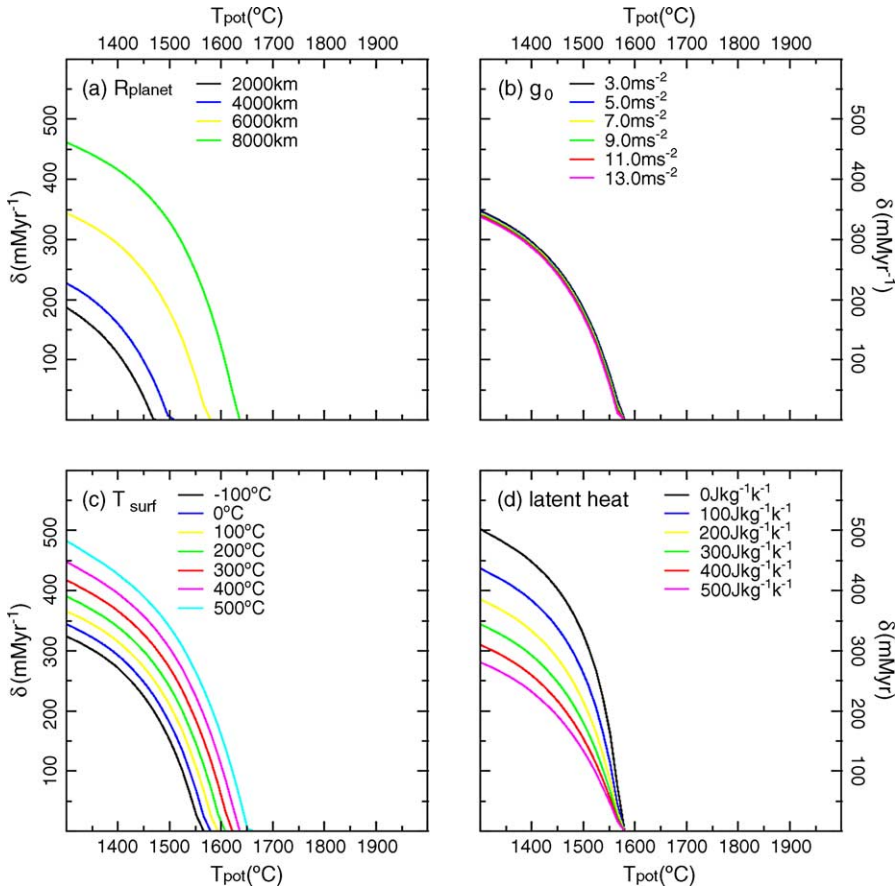


Fig. 13. Variation of the extrusion rate δ as a function of (a) planet size R_{planet} , (b) gravitational acceleration g_0 , (c) surface temperature T_0 , and (d) latent heat of melting ΔS . Values of non-varying parameters are $Q_{\text{core}} = 1 \text{ TW}$, $d_{\text{lith}} = 100 \text{ km}$, $H_0 = 4.8 \times 10^{-12} \text{ W kg}^{-1}$, $f = 0.80$, $-dT_{\text{pot}}/dt = 100 \text{ K G yr}^{-1}$, $g_0 = 7.0 \text{ ms}^{-2}$, $R = 6000 \text{ km}$, $\Delta S = 300 \text{ J kg}^{-1} \text{ K}^{-1}$. The core radius is half of the planetary radius in all cases. The potential to average temperature scaling factor $f_{T_{\text{avg}}}$ in Eq. (5) is recomputed for all different combinations of planet size and gravitational acceleration used.

presented $Ra-Nu$ models including melting, e.g. Hauck and Phillips, 2002), whereas in our extrusion model, advection is the primary heat transport mechanism in addition to conduction. We may nevertheless plot the associated thermal evolutions in our extrusion model results to consider the dynamical consequences of such thermal evolutions. For the stagnant lid $Ra-Nu$ models (Fig. 4b, blue curves for Earth/Venus, green curves for Mars), initial heating phases are observed in several cases, consistent with absence or low rates of volcanic activity in Figs. 10 and 12. In later stages, their positions in T_{pot} , dT_{pot}/dt -space in Fig. 12 (final temperatures of about 1370–1590 °C with cooling rates of about 60–80 K G yr⁻¹) would correspond to extrusion

rates of zero up to about 5–10 km³ yr⁻¹ for Mars and up to about 150 km³ yr⁻¹ for Venus.

4. Discussion

4.1. Plate tectonics on the early Earth

Many speculations about the nature of plate tectonics in a hotter Earth have been presented. They often involve faster spreading than in the present situation (e.g. Bickle, 1978, 1986) or a longer mid-ocean ridge system (e.g. Hargraves, 1986), to transport a greater heat flux from the mantle. Our results, however, show

that the hotter mantle itself generates the most important means of removing the increased heat flux from the mantle by thinning the lithosphere relative to a cooler mantle and thus significantly increasing the conductive heat flow through the lithosphere. This effect has also been noticed by Bickle (1978). If we compare the slope of the exponential model cooling curves of Fig. 4a in T_{pot} , dT_{pot}/dt -space (indicated in Fig. 6a–d by the shaded area) to the slope of the contours of equal turnover times, we observe that in all four models (Fig. 6a–d) the turnover time required for a certain cooling rate increases faster with potential temperature than the actual cooling rate predicted by the exponential cooling model for higher mantle temperatures. In other words, the exponential cooling curves predict a *slower* rate of operation for plate tectonics rather than a faster at higher mantle temperatures. This is consistent with the argument of Hargraves (1986), who predicts slower plate tectonics on the basis of reduced slab pull and ridge push forces in a hotter mantle. Only when cooling pulses at much higher cooling rate (see Fig. 5) than the exponential curve of Fig. 4a are considered will the turnover time τ be reduced to lower values at higher mantle temperatures during these periods of increased cooling. However, in between these pulses, the turnover time will be significantly larger than in the exponential cooling case. As we only have a rough idea of the cooling history of the Earth, it is difficult to place the different geological eras in the diagrams produced in this work. Several authors have shown that plate tectonics becomes increasingly more difficult in a hotter Earth (Sleep and Windley, 1982; Vlaar, 1986; Vlaar and Van den Berg, 1991; Davies, 1992; Van Thienen et al., 2004b) on the basis of lithospheric buoyancy, which may limit the applicability of our plate tectonics results on the high end of the T_{pot} spectrum.

4.2. Extrusion mechanism on the early Earth

The volumetric extrusion rates found in our models can be compared to extrusion rates representative of processes similar to the extrusion mechanism in the more recent Earth, like hotspots (i.e. areas of anomalous volcanism, Turcotte and Schubert, 2002) and flood volcanism. Hotspots typically have basalt production rates of 0.02 to 0.04 km³ yr⁻¹. Phanerozoic flood volcanism may have eruption rates two orders of mag-

nitude higher, about 0.75 to more than 1.5 km³ yr⁻¹ (Richards et al., 1989), with peak rates possibly up to 10 km³ yr⁻¹ (White and McKenzie, 1995) to possibly more than 100 km³ yr⁻¹ for the Ontong Java plateau (Coffin and Eldholm, 1994). These numbers are still smaller than the volumetric production rates up to $x \times 100$ km³ yr⁻¹ found in Fig. 10.

This means that if the mechanism played an important role in the cooling of the early Earth, much more extensive hotspot and flood volcanism activity may have been required to have sufficient cooling capacity. Much evidence is found for Archean and Proterozoic flood volcanism. Arndt (1999) discusses many occurrences all over the world. Abbott and Isley (2002) have identified a total of 62 superplume events and eras from the mid Archean to the present on the basis of flood basalts, dike swarms, high Mg rocks and layered intrusions, though especially for the Archean this is probably a lower limit because of preservation issues and lack of data. They estimate the original extent of the flood basalts generated by the separate events, using a correlation between maximum dike widths and flood basalt surface area. This approach is based on modeling work by Fialko and Rubin (1999), and was tested to five Phanerozoic flood basalt provinces for which accurate data for both maximum feeder dike width and flood basalt area were available, showing very good correlation ($R^2 = 0.99$, Abbott and Isley, 2002). For dike widths greater than 300 m (which is the maximum value in these five flood basalt provinces), some problems may occur in this relation pertaining to (possibly irregular) thermal erosion during magma transport. For this reason, Abbott and Isley (2002) limit the maximum dike width for huge Archean dikes to 1 km in their calculations. They find that both the magnitude and the frequency of these events was significantly higher during the late Archean and has declined since then. Abbott and Isley (2002) also identify six major events of which the estimated eruption volume of each was sufficient to cover at least 14–18% of the Earth's surface. When making an assumption about the average thickness of a flood basalt province, volumes can be computed and using estimated eruption times, volumetric eruption rates. In Table 4, estimates of eruption rates for four selected late Archean to early Proterozoic superplume events from Abbott and Isley (2002) have been calculated, using estimates for the average flood basalt thickness from Phanerozoic flood basalts

Table 4

Estimates of eruption rates for three different assumed flood basalt thicknesses d , based on areal extent estimates of superplume events by (Abbott and Isley, 2002, Table 8)

Duration (Myr)	Area (km ²)	Eruption rate (km ³ yr ⁻¹) $d = 1$ km	Eruption rate (km ³ yr ⁻¹) $d = 3$ km	Eruption rate (km ³ yr ⁻¹) $d = 5$ km
2409–2413	7.42×10^7	18.6	55.7	92.8
2433–2451	1.51×10^8	8.39	25.2	41.9
2582–2610	7.37×10^7	2.63	7.90	13.2
2899–2903	3.71×10^7	9.26	27.8	46.3

The average of the minimum and maximum areal extent reported by Abbott and Isley (2002) has been listed and used in calculating the eruption rates. The lowest two estimates for the average flood basalt thickness (1 and 3 km) are consistent with estimates of surface area and volume of several Phanerozoic flood basalts, listed in Table 1 of White and McKenzie (1995). We speculate that the higher value (5 km) may be more representative of larger scale events in the Archean.

(1–3 km, see Table 1 of White and McKenzie, 1995). The resulting numbers are of the same magnitude to up to one order of magnitude smaller than the eruption rates dictated by Fig. 10c–d (lower middle to right corner for moderate cooling rates at Archean mantle temperatures). However, if we extrapolate further back to the early/middle Archean, we may expect volumetric extrusion rates to be even higher for these events, and the number of up to about 350 km³ yr⁻¹ required by Fig. 10c–d for significant cooling rates is feasible with only a small number of active flood basalt provinces (last column of Table 4) for an early Earth that is only 150 K hotter than the present-day Earth (lower right corner of the shaded area in Fig. 10c and d).

For higher temperatures during the early history of the Earth, the required extrusion rate is smaller and therefore the required amount and activity of flood volcanism is smaller as well. For a hotter early Earth, say above 1750 °C, the numbers of Table 4 are similar to those in Fig. 10 and a single flood volcanism province may be sufficient, combined with global conductive cooling, to attain significant mantle cooling rates.

4.3. Cooling mechanisms of Mars

The results, shown in Fig. 8, clearly indicate that neither present nor early Mars requires plate tectonics to obtain considerable cooling rates on the order of 100 K G yr⁻¹ or more, and that the relatively small planet can cool conductively at considerable rates. Nimmo and Stevenson (2000) suggest that plate tectonics or some other efficient cooling agent was active during the first 500 Myr of the history of Mars, in order to allow the core heat flow to rise above the conductive level and initiate core convection, which

would produce a magnetic field of which the result is seen nowadays in the magnetization of some ancient Martian crustal rocks (Acuña et al., 1999). During this initial phase, the model results of Nimmo and Stevenson (2000) show an average cooling rate of about 400 K G yr⁻¹, combined with a core heat flux of about 1.3 TW (using their 1450 km core size). Although our Mars models use a core heat flux of 0.4 TW, Fig. 7 shows a low sensitivity of the results to variations in the core heat flux for Earth. For Mars, we expect the effect to be similarly small. Therefore, from the results of our model shown in Figs. 8b and 12b (early Mars) at a cooling rate of 400 K G yr⁻¹, we conclude that plate tectonics or basalt extrusion is not required to obtain this cooling rate at potential temperatures above 1700–1800 °C, since conductive cooling through the lithosphere is able to sustain this cooling rate by itself. Parametric models of Breuer and Spohn (2003) also indicate that a stagnant lid regime on early Mars may provide sufficient cooling to allow a dynamo (provided that the core is initially superheated), and their models suggest that this is more consistent with the history of crustal production on Mars than an early phase of plate tectonics. In other words, a significant contribution to the cooling of Mars by either plate tectonics or basalt extrusion is only to be expected when high cooling rates (>200 K G yr⁻¹) take place in a relatively cool early Mars ($T_{\text{pot}} < 1700\text{--}1800$ °C). This appears to be in contradiction with earlier work of Reese et al. (1998). Earlier work based on buoyancy considerations of oceanic lithosphere already showed that plate tectonics is only possible on Mars when it has a low potential temperature below 1300–1400 °C (Van Thienen et al., 2004b). Our new results add evidence to the unlikelihood of plate tectonics on Mars during its history. Our

models, however, do not take into account that in the reduced gravity of Mars, partial melting would generate a thick stratification of depleted, and therefore inherently less dense, mantle peridotite (Schott et al., 2001, 2002). This effect would possibly extend the thickness of the effective lithosphere, which we assume to coincide with our thermally defined lithosphere, to greater depths. This thickening of the lithosphere would decrease the required turnover time in the plate tectonics models, and increase the required volumetric eruption rate the extrusion models. Another effect that is not included in the calculations is that the use of a temperature and pressure dependent thermal conductivity rather than a constant value may significantly reduce the efficiency of conductive cooling through the lithosphere (Van den Berg and Yuen, 2002). There is plenty of evidence for an active volcanic history of Mars, the most important of which is the Tharsis region with its immense volcanoes. It is magmatic/volcanic of origin, and measures about $3 \times 10^8 \text{ km}^3$ of material (Zuber, 2001). Most volcanic and magmatic activity took place during the Noachian and Hesperian (Dohm and Tanaka, 1999), spanning a period from 4.57 Ga to an estimated 2.9 Ga (Hartmann and Neukum, 2001). The minimum volumetric eruption rate is obtained from the ratio of the volume and maximum formation time, which is less than $0.2 \text{ km}^3 \text{ yr}^{-1}$. Since the system was possibly

active for a shorter time, average eruption rates may have been higher, but the values probably remain low compared to for example the present day eruption rate at mid-ocean ridges of about $20 \text{ km}^3 \text{ yr}^{-1}$ (McKenzie and Bickle, 1988). Therefore, the magmatic activity involved in the formation of the Tharsis region probably did not have a strong effect on the cooling of Mars.

4.4. Cooling mechanisms of Venus

The results for present-day Venus for both mechanisms (Figs. 8c and 12c) show for the present estimated potential temperature of about $1300\text{--}1500 \text{ }^\circ\text{C}$ (Nimmo and McKenzie, 1998) that some activity is required from either plate tectonics or basalt extrusion even if *no cooling at all* takes place. This is consistent with earlier results of Reese et al. (1998). Magee and Head (2001) found from high-resolution radar images from the Magellan spacecraft that at least 9% of the planetary surface has been covered by large flow fields in the last several hundred million years. These flow fields are considered equivalents of flood basalts on Earth (Crumpler et al., 1997). The largest of these flow fields have areal extents comparable to those of the Deccan and Kerguelen provinces (Magee and Head, 2001; Abbott and Isley, 2002), and in total they measure $4.0 \times 10^7 \text{ km}^2$. Obviously, estimates of eruption rates as made for Earth

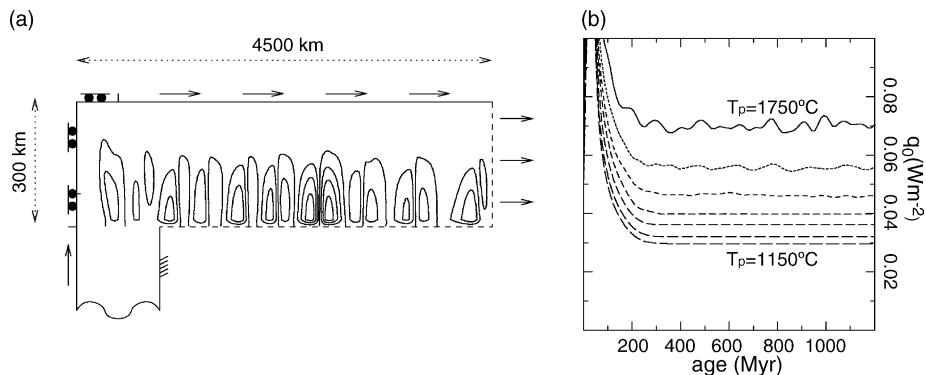


Fig. 14. (a) Numerical model setup. Adiabatic upwelling is prescribed in the left hand side limb of the model domain. A nonzero velocity is prescribed on (most of) the top boundary, corresponding to the plate velocity. Material leaves the domain through the right hand side boundary. The lower boundary of the long horizontal limb of the domain is open and kept at a temperature consistent with the potential temperature of the model. The viscosity is temperature and pressure dependent, using parameters from Karato and Wu (1993). Stream function contours indicate the instantaneous flow field at some time during one of the experiments. Small-scale sublithospheric convection is clearly visible. (b) Resulting surface heat flows for potential temperature of $1150 \text{ }^\circ\text{C}$ (long-dashed curve) up to $1750 \text{ }^\circ\text{C}$ (solid curve) in steps of $100 \text{ }^\circ\text{C}$. For these surface heat flows and potential temperatures, a plate thickness was sought that reproduces the surface heat flow in thermal equilibrium (far from the spreading ridge).

in Table 4 are more difficult to make because of unknown thicknesses and event durations. But for any thickness estimate up to several km, the average eruption rate over the last several hundred million years is well below $1 \text{ km}^3 \text{ yr}^{-1}$. The apparent virtual lack of volcanic and plate tectonic activity on the present-day Venus therefore indicates the position of the planet in the diagrams is below the horizontal axis, or that the planet is heating up. This has also been suggested by Turcotte (1995), Phillips and Hansen (1998), and Nimmo (2002).

Crater count statistics indicate an average age of the Venusian surface of about 300 million to 1 billion years (Schaber et al., 1992; McKinnon et al., 1997). At large there are two end-member interpretations of this remarkable feature. The first is that the planet underwent catastrophic global resurfacing and may be doing so periodically (Schaber et al., 1992; Strom et al., 1994). This type of behaviour may be illustrated by numerical convection models of Moresi and Solomatov (1998), in which brittle behaviour of the lithosphere results in its episodic catastrophic mobilization. An opposing view considers the young surface age to be caused by more or less constant resurfacing at a much lower pace (Phillips et al., 1992). However, from a statistical point of view, the data do not constrain either model (Campbell, 1999). Phillips and Hansen (1998) proposed a transition from a mobile lid regime prior to 700 Ma to a stagnant lid regime after 500 Ma. This range of models for the dynamical evolution of Venus allow very different cooling scenarios. In the more constant, non-episodic scenario, the thermal evolution of Venus may be expected to be close to the exponential cooling model of Fig. 4a. In an episodic dynamical scenario on the other hand, Venus can be expected to have been cooling during periods of increased activity, but our results suggest that during periods of inactivity, the planet's interior may have been heating up. This suggests that the episodic scenario for Venus results in a cyclicity in its thermal evolution (and one could speculate on the opposite effect, where sufficient mantle heating results in a new period of tectonic and/or volcanic activity). Turcotte (1993, 1995) suggested that Venus may have a history of periodic plate tectonics. From our results, plate tectonics and flood volcanism appear equally valid mechanisms of crustal production and heat loss in the cooling part of these hypothetical cycles.

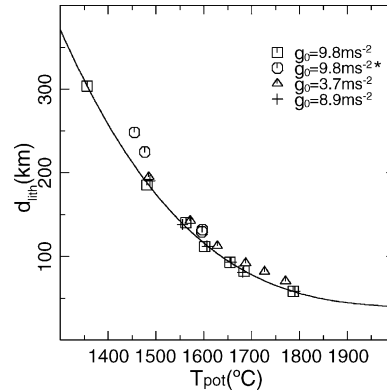


Fig. 15. Lithosphere thickness as a function of mantle potential temperature in a stagnant lid setting, obtained from numerical convection experiments (see text). Symbols represent experiments for Earth (squares), Earth with a larger model domain (circles, see text), Mars (triangles) and Venus (crosses) values of gravity. The cubic best fit of the Earth data, used in the extrusion models (Eq. (19)), is indicated by the solid curve.

We note that the results are not very sensitive to the surface temperature, which may have varied over several 100 K (Bullock and Grinspoon, 2001; Phillips et al., 2001), for relatively low mantle potential temperatures in the range of estimates for the present-day situation (1300–1500 °C Nimmo and McKenzie, 1998). For higher potential temperatures probably representative for the early history of Venus, the results are much more sensitive to surface temperature (see Figs. 9 and 13).

5. Conclusions

Our model results show that for a steadily (exponentially) cooling Earth, plate tectonics is capable of removing all the required heat at a plate tectonic rate comparable to or even lower than the current rate of operation. This is contrary to the notion that faster spreading would be required in a hotter Earth to be able to remove the extra heat (e.g. Bickle, 1978). However, whether or not plate tectonics could work on any planet significantly hotter than present-day Earth is another question, which is addressed elsewhere (Sleep and Windley, 1982; Vlaar, 1985; Vlaar and Van den Berg, 1991; Van Thienen et al., 2004b). In the early Earth, the extrusion mechanism was probably more important, as indicated by ubiquitous flood basalts in the

Archean (Arndt, 1999). For this mechanism to be able to contribute a significant part to the cooling of the Earth at rates comparable to the present rate of cooling, eruption rates up to one to two orders of magnitude higher than for Phanerozoic flood basalts are required. However, this is consistent with the increase in both frequency and magnitude of flood volcanism towards the Archean (Abbott and Isley, 2002). Mars seems to be capable of cooling conductively through its lithosphere without either plate tectonics or flood volcanism at significant cooling rates, due to its small size and, as a consequence, large surface to volume ratio. Only in hypothetical episodes of rapid cooling ($>200 \text{ K G yr}^{-1}$) during the early history of Mars, some additional mechanism may have been active, which can be either plate tectonics or flood volcanism. We confirm the inference of earlier papers (Turcotte, 1995; Phillips and Hansen, 1998; Nimmo, 2002) that the mantle of Venus is heating up. When assuming an episodic history for Venus (e.g. Turcotte, 1995), our results suggest a cyclicity of mantle heating and cooling. Throughout its history, with the possible exception of the earliest, presumably hottest phase due to uncertainties in the surface temperature, this planet has required a mechanism additional to conduction for the cooling of its interior, operating at rates comparable to those of the Earth.

Acknowledgments

We thank Michel Jacobs for discussions relating to material properties of mantle materials, and W. Moore, S. Hauck II, and two anonymous reviewers for useful and constructive comments which helped to significantly improve the paper. Peter van Thienen acknowledges the financial support provided through the European Community's Human Potential Programme under contract RTN2-2001-00414, MAGE.

Appendix A. Parameterization of plate thickness in the plate tectonics model

A finite element mantle convection code (see Van den Berg et al., 1993) was used in a series of experiments designed to obtain a relation between the mantle potential temperature and the effective plate thickness in a plate tectonic regime. The experimental setup for the model is indicated in Fig. 14a. Upwelling is pre-

scribed in the left hand side limb of the model domain. A nonzero velocity corresponding to the plate velocity is prescribed on (most of) the top boundary. A relatively low half spreading rate of about 4 mm/yr is used to limit the length of lithosphere required to reach thermal equilibrium. Material leaves the domain through the right hand side boundary with the prescribed plate velocity. The lower boundary of the long horizontal limb of the domain is open and kept at a temperature consistent with the potential temperature of the model, allowing relatively warm material to rise into the domain and cold material to sink out of the domain. The viscosity is temperature and pressure dependent, using parameters from Karato and Wu (1993) halfway between their wet and dry parameters. We determined the surface heat flow for the steady state part of the lithosphere (far from the ridge, see Fig. 14b). Through trial-and-error, we searched for an effective plate thickness y_{LO} in Eq. (6) to match the heat flow at the potential temperature of each model characterized by the value of the potential temperature T_{pot} . Because the models are kinematically driven, buoyancy is of minor importance and the results are insensitive to gravitational acceleration and therefore applicable to Mars and Venus as well. Second-order motion in the form of small-scale sublithospheric convection (see Parsons and Sclater, 1977; Sleep, 2002) may be different on the different planets due to possible differences in gravitational acceleration and mantle viscosity. As a consequence of the different gravity, the Rayleigh number describing this process will be a factor 2.5 smaller for Mars than for Earth (since $g_0^{Mars} \approx 0.4 \times g_0^{Earth}$), the effect of which is relatively minor. The Rayleigh number inversely with mantle viscosity, which may therefore be of greater importance. However, the mantle viscosities of Mars and Venus are not well constrained, but may be higher due to a possibly lower water content, which would cause a greater effective plate thickness. We assume the effective plate thickness parameterization obtained for Earth-like parameters to be valid for Mars and Venus as well, keeping this caveat in mind.

Appendix B. Parameterization of lithosphere thickness in the extrusion model

Heating is only internal (zero bottom heat flux), and a zero temperature is prescribed on the top boundary.

Side boundaries are periodic. The domain has a depth of 670 km, an aspect ratio of 1.5, a no-slip top boundary and a free slip bottom boundary. A series of models with different internal heating rates was started to generate a range of statistical steady state potential temperatures and lithospheric thicknesses. For each model, the lithospheric thickness, represented by the depth of the 1327 °C isotherm is plotted against the potential temperature and a fit is computed for the entire set (see Fig. 15), see expression (19).

Since these models are not kinematically driven but are convecting actively, we have done the experiments for different values for the gravitational acceleration, representing the different planets (see Table 2). As can be seen in Fig. 15, the results of the experiments described above applied to Mars and Venus (in which the gravitational acceleration is the control parameter) nearly coincide with the best fit curve for Earth, so this curve is used for all planets (the possibly higher mantle viscosities for Venus and Mars, which would cause an increase in the lithosphere thickness, are kept in mind). We have tested the sensitivity of this result to the depth of the domain, rerunning several experiments with a doubled width and depth. Resulting lithosphere thicknesses are slightly greater but of comparable magnitude (see Fig. 15).

References

- Abbott, D.H., Isley, A.E., 2002. The intensity, occurrence and duration of superplume events and eras over geological time. *J. Geodyn.* 34, 265–307.
- Acuña, M.H., Connery, J.E.P., Ness, N.F., Lin, R.P., Mitchell, D., Carlson, C.W., McFadden, J., Anderson, K.A., Rème, H., Mazelle, C., Vignes, D., Wazilewsky, P., Cloutier, P., 1999. Global distribution of crustal magnetization discovered by the Mars global surveyor MAG/ER experiment. *Science* 284 (5415), 790–793.
- Anderson, O.L., 2002. The power balance at the core-mantle boundary. *Phys. Earth Planet. Inter.* 131, 1–17.
- Arndt, N., 1999. Why was flood volcanism on submerged continental platforms so common in the Precambrian?. *Precambrian Res.* 97, 155–164.
- Ballard, S., Pollack, H.N., 1987. Diversion of heat by Archean cratons: a model for southern Africa. *Earth Plan. Sci. Lett.* 85, 253–264.
- Ballard, S., Pollack, H.N., 1988. Modern and ancient geotherms beneath southern Africa. *Earth Plan. Sci. Lett.* 88, 132–142.
- Bickle, M.J., 1978. Heat loss from the Earth: a constraint on Archean tectonics from the relation between geothermal gradients and the rate of plate production. *Earth Plan. Sci. Lett.* 40, 301–315.
- Bickle, M.J., 1986. Implications of melting for stabilisation of the lithosphere and heat loss in the Archean. *Earth Plan. Sci. Lett.* 80, 314–324.
- Breuer, D., Spohn, T., 2003. Early plate tectonics versus single-plate tectonics on Mars: evidence from magnetic field history and crust evolution. *J. Geophys. Res.* 108 (E7).
- Buffett, B.A., 2003. The thermal state of the Earth's core. *Science* 299 (5613), 1675–1676.
- Bullock, M.A., Grinspoon, D.H., 2001. The recent evolution of climate on Venus. *Icarus* 150, 19–37.
- Campbell, B.A., 1999. Surface formation rates and impact crater densities on Venus. *J. Geophys. Res.* 104 (E9), 21,951–21,955.
- Carlsaw, H.S., Jaeger, J.C., 1959. *Conduction of Heat in Solids*. Clarendon Press, Oxford.
- Christensen, U.R., 1985. Thermal evolution models for the earth. *J. Geophys. Res.* 90 (B4), 2995–3007.
- Coffin, M.F., Eldholm, O., 1994. Large igneous provinces: crustal structure, dimensions, and external consequences. *Rev. Geophys.* 32, 1–36.
- Crumpler, L.S., Aubele, J.C., Senske, D.A., Keddie, S.T., Magee, K.P., Head, J.W., 1997. Volcanoes and centers of volcanism on Venus. In: Bougher, S.W., Hunten, D.M., Phillips, R.J. (Eds.), *Venus II. Geology, Geophysics, Atmosphere, and Solar Wind Environment*. University of Arizona Press, pp. 697–756.
- Davies, G.F., 1979. Thickness and thermal history of continental crust and root zones. *Earth Plan. Sci. Lett.* 44, 231–238.
- Davies, G.F., 1980. The histories of convective Earth models and constraints on radiogenic heat production in the Earth. *J. Geophys. Res.* 85 (B5), 2517–2530.
- Davies, G.F., 1992. On the emergence of plate tectonics. *Geology* 20, 963–966.
- De Wit, M.J., 1998. On Archean granites, greenstones, cratons and tectonics: does the evidence demand a verdict? *Precambrian Res.* 91, 181–226.
- Dohm, J.D., Tanaka, K.L., 1999. Geology of the Thaumasia region, Mars: plateau development, valley origins, and magmatic evolution. *Planetary and Space Science* 47, 411–431.
- Doin, M.P., Fleitout, L., 1996. Thermal evolution of the oceanic lithosphere: an alternative view. *Earth Plan. Sci. Lett.* 142, 121–136.
- Dumoulin, C., Doin, M.-P., Fleitout, L., 2001. Numerical simulation of the cooling of an oceanic lithosphere above a convective mantle. *Earth Plan. Sci. Lett.* 125, 45–64.
- Fei, Y., Moa, H., Mysen, B.O., 1991. Experimental determination of element partitioning and calculation of phase relations in the MgO–FeO–SiO₂ system at high pressure and high temperature. *J. Geophys. Res.* 96, 2157–2169.
- Fialko, Y.A., Rubin, A.M., 1999. Thermal and mechanical aspects of magma emplacement in giant dike swarms. *J. Geophys. Res.* 104 (B10).
- Folkner, W.M., Yoder, C.F., Yuan, D.N., Standish, E.M., Preston, R.A., 1997. Interior structure and seasonal mass redistribution of Mars from radio tracking of Mars Pathfinder. *Science* 278, 1749–1751.

- Hamilton, W.B., 1998. Archean magmatism and deformation were not products of plate tectonics. *Precambrian Res.* 91, 143–179.
- Hargraves, R.B., 1986. Faster spreading or greater ridge length in the Archean? *Geology* 14, 750–752.
- Hartmann, W.K., Neukum, G., 2001. Cratering chronology and the evolution of Mars. *Space Science Rev.* 96, 165–194.
- Hauck, S.A.I., Phillips, R.J., 2002. Thermal and crustal evolution of Mars. *J. Geophys. Res.* 107 (E7).
- Head, J.W.I., Coffin, M.F., 1997. Large Igneous Provinces: a planetary perspective. In: Mahoney, J.J., Coffin, M.F. (Eds.), *Large Igneous Provinces: Continental, Oceanic, and Planetary Flood Volcanism*. American Geophysical Union, Washington, DC, pp. 411–438.
- Hofmeister, A., 1999. Mantle values of thermal conductivity and the geotherm from phonon lifetimes. *Science* 283, 1699–1706.
- Honda, S., Iwase, Y., 1996. Comparison of the dynamic and parameterized models of mantle convection including core cooling. *Earth Plan. Sci. Lett.* 139, 133–145.
- Honda, S., Yuen, D.A., 2001. Interplay of variable thermal conductivity and expansivity on the thermal structure of oceanic lithosphere. *Geophys. Res. Lett.* 28 (2), 351–354.
- Juteau, T., Maury, R., 1999. *The Oceanic Crust, from Accretion to Mantle Recycling*. Springer-Praxis.
- Karato, S.-I., Wu, P., 1993. Rheology of the upper mantle: a synthesis. *Science* 260, 771–778.
- King, S.D., Anderson, D.L., 1995. An alternative mechanism of flood basalt formation. *Earth Plan. Sci. Lett.* 36 (3–4), 269–279.
- Kusky, T.M., 1998. Tectonic setting and terrane accretion of the Archean Zimbabwe craton. *Geology* 26 (2), 163–166.
- Kusky, T.M., Li, J.-H., Tucker, R.D., 2001. The Archean Dongwanzi ophiolite complex, North China craton: 2.505-billion-year-old oceanic crust and mantle. *Science* 292, 1142–1145.
- Labrosse, S., 2002. Hotspots, mantle plumes and core heat loss. *Earth Plan. Sci. Lett.* 199, 147–156.
- Labrosse, S., Poirier, J.-P., Le Mouél, J.-L., 1997. On cooling of the earth's core. *Phys. Earth Planet. Inter.* 99, 1–17.
- Magee, K.P., Head, J.W., 2001. Large flow fields on Venus: implications for plumes, rift associations, and resurfacing. In: Ernst, R.E., Buchan, K.L. (Eds.), *Mantle Plumes: their Identification Through Time*. Geological Society of America, Boulder, Colorado, pp. 81–101, GSA special paper 352.
- McCulloch, M.T., Bennett, V.C., 1994. Progressive growth of the Earth's continental crust and depleted mantle: geochemical constraints. *Geochim. Cosmochim. Acta* 58 (21), 4717–4738.
- McKenzie, D.P., 1967. Some remarks on heat flow and gravity anomalies. *J. Geophys. Res.* 72 (24), 6261–6273.
- McKenzie, D.P., Bickle, M.J., 1988. The volume and composition of melt generated by extension of the lithosphere. *J. Petrology* 29, 625–679.
- McKinnon, W.B., Zahnle, K.J., Ivanov, B.A., Melosh, H.J., 1997. Cratering on Venus: models and observations. In: Bougher, S.W., Hunten, D.M., Phillips, R.J. (Eds.), *Venus II, Arizona*. The University of Arizona Press.
- Monnereau, M., Dubuffet, F., 2002. Is Io's mantle really molten? *Icarus* 158, 450–459.
- Moresi, L., Solomatov, V., 1998. Mantle convection with a brittle lithosphere: thoughts on the global tectonic styles of the Earth and Venus. *Geophys. J. Int.* 133, 669–682.
- Nimmo, F., 2002. Why does Venus lack a magnetic field? *Geology* 30 (11), 987–990.
- Nimmo, F., McKenzie, D., 1996. Modelling plume-related uplift, gravity and melting on Venus. *Earth Plan. Sci. Lett.* 145, 109–123.
- Nimmo, F., McKenzie, D., 1998. Volcanism and tectonics on Venus. *Ann. Rev. Earth Planet. Sci.* 26, 23–51.
- Nimmo, F., Stevenson, D.J., 2000. Influence of early plate tectonics on the thermal evolution and magnetic field of Mars. *J. Geophys. Res.* 105 (E5), 11,969–11,979.
- Nisbet, E.G., Cheadle, M.J., Arndt, N.T., Bickle, M.J., 1993. Constraining the potential temperature of the Archean mantle: a review of the evidence from komatiites. *Lithos* 30, 291–307.
- Oxburgh, E.R., Parmentier, E.M., 1977. Compositional and density stratification in oceanic lithosphere - causes and consequences. *J. Geol. Soc. Lond.* 133, 343–355.
- Parmentier, E.M., Hess, P.C., 1992. Chemical differentiation of a convecting planetary interior: consequences for a one plate planet such as Venus. *Geophys. Res. Lett.* 19 (20), 2015–2018.
- Parsons, B., Sclater, J.G., 1977. An analysis of the variation of ocean floor bathymetry and heat flow with age. *J. Geophys. Res.* 82 (B5), 803–827.
- Phillips, R.J., Bullock, M., Hauck II, S., 2001. Climate and interior coupled evolution on Venus. *Geophys. Res. Lett.* 28, 1779–1782.
- Phillips, R.J., Hansen, V.L., 1998. Geological evolution of Venus: rises, plains, plumes, and plateaus. *Science* 279, 1492–1497.
- Phillips, R.J., Raubertas, R.F., Arvidson, R.E., Sarkar, I.C., Herrick, R.R., Izenberg, N., Grimm, R.E., 1992. Impact craters and Venus resurfacing history. *J. Geophys. Res.* 97 (E10), 15,923–15,948.
- Pollack, H.N., Hurter, S.J., Johnson, J.R., 1993. Heat flow from the Earth's interior: analysis of the global data set. *Rev. of Geophysics* 31 (3), 267–280.
- Reese, C.C., Solomatov, V.S., Moresi, L.-N., 1998. Heat transport efficiency for stagnant lid convection with dislocation viscosity: application to Mars and Venus. *J. Geophys. Res.* 103 (E6), 13,643–13,657.
- Richards, M.A., Duncan, R.A., Courtillot, V.E., 1989. Flood basalts and hot-spot tracks: plume heads and tails. *Science* 246, 103–107.
- Sanloup, C., Jambon, A., Gillet, P., 1999. A simple chondritic model of Mars. *Phys. Earth Planet. Inter.* 112, 43–54.
- Saxena, S., 1996. Earth mineralogical mode: Gibbs free energy minimization computation in the system MgO–FeO–SiO₂. *Geochim. Cosmochim. Acta* 60, 2379–2395.
- Schaber, G.G., Strom, R.G., Moore, H.J., Soderblom, L.A., Kirk, R.L., Chadwick, D.J., Dawson, D.D., Gaddis, L.R., Boyce, J.M., Russel, J., 1992. Geology and distribution of impact craters on Venus: what are they telling us?. *J. Geophys. Res.* 97 (E8), 13,257–13,301.
- Schott, B., Van den Berg, A.P., Yuen, D.A., 2001. Focussed time-dependent Martian volcanism from chemical differentiation coupled with variable thermal conductivity. *Geophys. Res. Lett.* 28 (22), 4271–4274.
- Schott, B., Van den Berg, A. P., Yuen, D. A., 2002. Slow secular cooling and long lived volcanism on Mars

- explained. Lunar and Planetary Science Conference 33. <http://www.lpi.usra.edu/meetings/lpsc2002>.
- Schubert, G., Spohn, T., 1990. Thermal history of Mars and the sulfur content of its core. *J. Geophys. Res.* 95 (B9), 14,095–14,104.
- Slater, J.G., Jaupart, C., Galson, D., 1980. The heat flow through oceanic and continental crust and the heat loss of the Earth. *Rev. Geophys. Space Phys.* 18 (1), 269–311.
- Sharpe, H.N., Peltier, W.R., 1978. Parameterized mantle convection and the Earth's thermal history. *Geophys. Res. Lett.* 5 (9), 737–740.
- Sleep, N.H., 1990. Hotspots and mantle plumes: some phenomenology. *J. Geophys. Res.* 95 (B5), 6715–6736.
- Sleep, N.H., 2002. Local lithospheric relief associated with fracture zones and ponded plume material. *Geochem. Geophys. Geosyst.* 3 (12).
- Sleep, N.H., Windley, B.F., 1982. Archean plate tectonics: constraints and inferences. *J. Geol.* 90, 363–379.
- Snyder, D., 2002. Cooling of lava flows on Venus: the coupling of radiative and convective heat transfer. *J. Geophys. Res.* 107. doi:10.1029/2001JE001501.
- Solomatov, V.S., Moresi, L.-N., 1996. Stagnant lid convection on Venus. *J. Geophys. Res.* 101 (E2), 4737–4753.
- Solomatov, V.S., Moresi, L.-N., 2000. Scaling of time-dependent stagnant lid convection: application to small-scale convection on earth and other terrestrial planets. *J. Geophys. Res.* 105 (B9), 1,795–21,817.
- Solomatov, V.S., Zharkov, V.N., 1990. The thermal regime of Venus. *Icarus* 84, 280–295.
- Spohn, T., Schubert, G., 1982. Modes of mantle convection and the removal of heat from the earth's interior. *J. Geophys. Res.* 87 (B6) 4682–4696.
- Stein, C.A., Stein, S., 1992. A model for the global variation in oceanic depth and heat flow with lithospheric age. *Nature* 359, 123–129.
- Stevenson, D.J., Spohn, T., Schubert, G., 1983. Magnetism and thermal evolution of the terrestrial planets. *Icarus* 54, 466–489.
- Stixrude, L., Cohen, R.E., 1993. Stability of orthorhombic MgSiO₃ perovskite in the earth's lower mantle. *Nature* 364 (6438), 613–636.
- Strom, R.G., Schaber, G.G., Dawson, D.D., 1994. The global resurfacing of Venus. *J. Geophys. Res.* 99 (E5), 10,899–10,926.
- Turcotte, D.L., 1980. On the thermal evolution of the earth. *Earth Plan. Sci. Lett.* 48, 53–58.
- Turcotte, D.L., 1993. An Episodic Hypothesis for Venusian Tectonics. *J. Geophys. Res.* 98 (E9), 17,061–17,068.
- Turcotte, D.L., 1995. How does Venus lose heat? *J. Geophys. Res.* 100 (E8), 16931–16940.
- Turcotte, D.L., Schubert, G., 2002. Geodynamics, Applications of continuum physics to geological problems, Second ed. John Wiley & Sons.
- Vacquier, V., 1998. A theory of the origin of the Earth's internal heat. *Tectonophysics* 291, 1–7.
- Van den Berg, A. P., Rainey, E. S. G., Yuen, D. A., 2004. The combined influence of variable thermal conductivity, temperature- and pressure-dependent viscosity and core-mantle coupling on thermal evolution. *Phys. Earth Planet. Inter.* in press.
- Van den Berg, A.P., Van Keken, P.E., Yuen, D.A., 1993. The effects of a composite non-Newtonian and Newtonian rheology on mantle convection. *Geophys. J. Int.* 115, 62–78.
- Van den Berg, A.P., Yuen, D.A., 2002. Delayed cooling of the earth's mantle due to variable thermal conductivity and the formation of a low conductivity zone. *Earth Plan. Sci. Lett.* 199, 403–413.
- Van den Berg, A.P., Yuen, D.A., Allwardt, J.R., 2002. Non-linear effects from variable thermal conductivity and mantle internal heating: implications for massive melting and secular cooling of the mantle. *Phys. Earth Planet. Inter.* 129, 359–375.
- Van Thienen, P., Van den Berg, A.P., Vlaar, N.J., 2004a. Production and recycling of oceanic crust in the early earth. *Tectonophysics* 386 (1–2), 41–65.
- Van Thienen, P., Vlaar, N.J., Van den Berg, A.P., 2004b. Plate tectonics on the terrestrial planets. *Phys. Earth Planet. Inter.* 142 (1–2), 61–74.
- Vlaar, N.J., 1985. Precambrian geodynamical constraints. In: Tobi, A.C., Touret, J.L.R. (Eds.), *The Deep Proterozoic Crust in the North Atlantic Provinces*, pp. Reidel 3–20.
- Vlaar, N.J., 1986. Archaean global dynamics. *Geologie en Mijnbouw* 65, 91–101.
- Vlaar, N.J., Van den Berg, A.P., 1991. Continental evolution and archaeo-sea-levels. In: Sabadini, R., Lambeck, K., Boschi, E. (Eds.), *Glacial Isostasy, Sea-Level and Mantle Rheology*. Kluwer, Dordrecht, The Netherlands.
- Vlaar, N.J., Van Keken, P.E., Van den Berg, A.P., 1994. Cooling of the Earth in the Archaean: consequences of pressure-release melting in a hotter mantle. *Earth Plan. Sci. Lett.* 121, 1–18.
- White, R.S., McKenzie, D., 1995. Mantle plumes and flood basalts. *J. Geophys. Res.* 100 (B9), 17543–17585.
- Williams, J.-P., Paige, D.A., Manning, C.E., 2003. Layering in the wall rock of Valles Marineris: intrusive and extrusive magmatism. *Geophys. Res. Lett.* 30 (12).
- Yoder, C.F., Konoplic, A.S., Yuan, D.N., Standish, E.M., Folkner, W.M., 2003. Fluid core size of Mars from detection of the solar tide. *Science* 300, 299–303.
- Yukutake, T., 2000. The inner core and the surface heat flow as clues to estimating the initial temperature of the earth's core. *Phys. Earth Planet. Inter.* 121, 103–137.
- Zhai, M., Zhao, G., Zhang, Q., 2002. Is Dongwanzi Complex an Archean Ophiolite? *Science* 295 (5557), 923.
- Zhang, C.Z., Zhang, K., 1995. On the internal structure and magnetic fields of Venus. *Earth, Moon Planets* 69, 237–247.
- Zuber, M.T., 2001. The crust and mantle of Mars. *Nature* 412, 220–227.